Journal of Computational Neuroscience (2021) 49:229–249
https://doi.org/10.1007/s10827-020-00760-7

Frontal eye field inactivation alters the readout of superior colliculus activity for saccade generation in a task-dependent manner

Tyler R. Peel[1] · Suryadeep Dash[2,3] · Stephen G. Lomber[4] · Brian D. Corneil[2,3,5,6]

Received: 16 February 2020 / Revised: 16 July 2020 / Accepted: 24 July 2020 / Published online: 8 November 2020

Abstract

Saccades require a spatiotemporal transformation of activity between the intermediate layers of the superior colliculus (iSC) and downstream brainstem burst generator. The dynamic linear ensemble-coding model (Goossens and Van Opstal 2006) proposes that each iSC spike contributes a fixed mini-vector to saccade displacement. Although biologically-plausible, this model assumes cortical areas like the frontal eye fields (FEF) simply provide the saccadic goal to be executed by the iSC and brainstem burst generator. However, the FEF and iSC operate in unison during saccades, and a pathway from the FEF to the brainstem burst generator that bypasses the iSC exists. Here, we investigate the impact of large yet reversible inactivation of the FEF on iSC activity in the context of the model across four saccade tasks. We exploit the overlap of saccade vectors generated when the FEF is inactivated or not, comparing the number of iSC spikes for metrically-matched saccades. We found that the iSC emits fewer spikes for metrically-matched saccades during FEF inactivation. The decrease in spike count is task-dependent, with a greater decrease accompanying more cognitively-demanding saccades. Our results show that FEF integrity influences the readout of iSC activity in a task-dependent manner. We propose that the dynamic linear ensemble-coding model be modified so that FEF inactivation increases the gain of a readout parameter, effectively increasing the influence of a single iSC spike. We speculate that this modification could be instantiated by FEF and iSC pathways to the cerebellum that could modulate the excitability of the brainstem burst generator.

Keywords Frontal eye field · Reversible inactivation · Superior colliculus · Saccade · Spatiotemporal transformation · Oculomotor system

This article belongs to the Topical Collection: *Vision and Action*
Guest Editors: Aasef Shaikh and Jeffrey Shall

Action Editor: Aasef G. Shaikh

Significance statement
One of the enduring puzzles in the oculomotor system is how it achieves the spatiotemporal transformation, converting spatial activity within the intermediate layers of the superior colliculus (iSC) into a rate code within the brainstem burst generator. The spatiotemporal transformation has traditionally been viewed as the purview of the oculomotor brainstem. Here, within the context of testing a biologically-plausible model of the spatiotemporal transformation, we show that reversible inactivation of the frontal eye fields (FEF) decreases the number of spikes issued by the iSC for metrically-matched saccades, with greater decreases accompanying more cognitively-demanding tasks. These results show that signals from the FEF influence the spatiotemporal transformation.

✉ Brian D. Corneil
bcorneil@uwo.ca

[1] Département de neurosciences, Université de Montréal, Montréal, QC, Canada

[2] The Brain and Mind Institute, University of Western Ontario, London, Ontario, Canada

[3] Department of Physiology & Pharmacology, University of Western Ontario, London, ON, Canada

[4] Department of Psychology, McGill University, Montréal, QC, Canada

[5] Department of Psychology, University of Western Ontario, London, ON, Canada

[6] Robarts Research Institute, 1151 Richmond St N, London, ON N6A 5B7, Canada

1 Introduction

The intermediate layers of the superior colliculus (iSC) are a key midbrain structure for generating saccadic eye movements, with the location of activity specifying the intended saccade vector (Gandhi and Katnani 2011; Sparks 2002; White and Munoz 2011). Downstream of the iSC, this spatial code is transformed into a temporal code, wherein the horizontal and vertical components of saccade displacement relate to the duration of recruitment of the brainstem burst generator. Importantly, it has also been long known that the level of iSC activation within its spatial map predicts the velocity of the ensuing saccadic eye movement (Nichols and Sparks 1996; Smalianchuk et al. 2018; Sparks and Mays 1990), although the neuronal mechanism for this dual-coding hypothesis has remained elusive. Goossens and Van Opstal (2006) proposed a dynamic linear ensemble-coding model that provides a novel mechanism for the spatiotemporal transformation of iSC activity. In this model, each iSC spike contributes a fixed site-specific mini-vector to saccade displacement, so that the cumulative spike count monotonically increases along the intended saccade vector. In support of this model, the iSC emits an invariant number of spikes even during displacement-matched saccades that exhibit highly-perturbed kinematics due to an induced blink (Goossens and Van Opstal 2006). This spike invariant model also explains the non-linear main sequence relationship of peak saccade velocity to saccade amplitude *via* logarithmic coding of oculomotor space within the iSC and the associated rostral-caudal gradient of the temporal burst profiles of iSC neurons (Goossens and Van Opstal 2012; Van der Willigen et al. 2011; Van Opstal and Goossens 2008). More recently, Kasap and Van Opstal (2017, 2019) simulated the dynamics of iSC activity using a neural network model, and found that the inclusion of lateral synaptic interactions within the iSC produce plausible profiles of iSC activity once triggered by an external input, subsequently generating realistic saccades. This implies that once a saccade vector is specified, the iSC and downstream brainstem burst generator instantiate the spatiotemporal transformation for saccade generation.

Given that the vast majority of neurophysiology evidence suggests that the iSC is the key convergence area of spatial information for saccade preparation (Gandhi and Katnani 2011; Hanes and Wurtz 2001; Sparks 1986; Wurtz et al. 2001), most models of the spatiotemporal transformation, including the dynamic linear ensemble coding model, have considered the role of cortical areas only from the perspective of specifying the intended saccade target. However, the iSC and other cortical (*e.g.*, frontal eye fields; FEF, lateral intraparietal area) and subcortical (*e.g.*, basal ganglia and cerebellum) areas have direct or indirect connections to each other that are active during saccade generation (Barash et al. 1991; Bruce and Goldberg 1985; Crapse and Sommer 2009; Fuchs et al. 1993; Hikosaka et al. 2000; Wurtz et al. 2001). The FEF is particularly important, as its integrity is critical for saccade generation if the iSC has been permanently ablated or reversibly inactivated (Keating and Gooley 1988; Schiller et al. 1980), presumably *via* FEF projections to the oculomotor brainstem that bypass the iSC (Segraves 1992) and/or *via* FEF projections through the midbrain nucleus reticularis tegmenti pontis (NRTP) to influence cerebellar circuits (Quaia et al. 1999; Xiong et al. 2002). These considerations have led us to wonder if a core prediction of the dynamic linear ensemble coding model, which is the generation of an invariant number of iSC spikes for saccades, would hold when the FEF is suddenly inactivated. Considering that FEF inactivation prolongs saccade duration (Peel et al. 2014), this examination of iSC activity without FEF inputs provides an ideal situation to test the dual-coding aspects of the model, especially in those tasks implicated with FEF function. Although we are testing this prediction in the context of the dynamic linear ensemble coding model, we may well make observations pertinent to other models of spatiotemporal transformations.

In a recent series of studies, we have recorded iSC activity while reversibly inactivating the FEF with cryogenic cooling probes (Dash et al. 2018; Peel et al. 2017). This allowed us to examine the impact of a sudden decrease in FEF input while recording the same iSC neuron. Here, we test whether FEF inactivation alters the cumulative spike count in the iSC neurons, primarily focusing our analyses on trials with displacement-matched saccades that control for any hypometria induced by FEF inactivation. We do this across four different saccade tasks, since the impact of FEF inactivation on saccade kinematics increases for more cognitively-demanding tasks (Deng et al. 1986; Dias and Segraves 1999; Peel et al. 2014; Sommer and Tehovnik 1997). We find that FEF inactivation reduced the number of spikes for displacement-matched saccades across our sample of iSC neurons, with larger reductions accompanying more cognitively-demanding tasks. Importantly, the decrease in spike count extended throughout the saccade-related response field for a given iSC neuron, doing so in a manner that altered how the instantaneous number of iSC spikes related to saccade displacement. Fundamentally, the iSC emitted fewer spikes during FEF inactivation. These results demonstrate that signals from the FEF influence the readout of iSC activity by the brainstem burst generator, which we surmise relates to the excitability of the brainstem burst generator.

2 Methods

This manuscript is partly based on experimental data reported in two previous studies (Dash et al. 2018; Peel et al. 2017), which characterized the effects of cryogenic FEF inactivation on iSC activity in immediate and delayed saccade tasks,

respectively (Experiment 1). We also carried out novel experiments to address how FEF inactivation altered saccade-related response fields in the iSC (Experiment 2).

2.1 Experimental procedures

Data was obtained from two male monkeys (*Macaca mulatta*, monkeys D, and O weighing 9.8, and 8.6 kg respectively) for each experiment. As previously described (Peel et al. 2017), each monkey underwent two surgeries to permit extracellular recordings from the iSC, and cryogenic inactivation of the FEF using cryoloops implanted into the arcuate sulcus. All training, surgical, and experimental procedures conformed to the policies of the Canadian Council on Animal Care and National Institutes of Health on the care and use of laboratory animals, and were approved by the Animal Use Subcommittee of the University of Western Ontario Council on Animal Care. We monitored the monkeys' weights daily and their health was under the close supervision of the university veterinarians.

For each experiment, we recorded extracellular activity of an isolated iSC neuron pre-, peri-, and post-cooling of the FEF while monkeys performed a saccade task. Eye position signals were sampled using a single, chair-mounted eye tracker at 500 Hz (EyeLink II). All neurons were recorded ~1 mm or more below the surface of the SC, in locations where electrical stimulation (300 Hz, 100 ms, biphasic cathodal-first pulses with each phase 0.3 ms in duration) evoked saccades with currents <50 μA. In the first experiment, potential cue locations were at the center of a neuron's response field and at the diametrically opposition position. We approximated the center of a given neuron's response field by identifying the saccade vector associated with the highest firing rates before FEF inactivation. To quantify the changes across the response field with FEF inactivation, we also conducted a second experiment wherein we recorded iSC neurons while monkeys performed saccades towards cues dispersed throughout the response field. We specified the number and spacing of cues (averages of 49 and 3°, respectively) within a square grid to sample the extent of a given neuron's response field.

After completion of the pre-cooling session (~60 trials for each session), chilled methanol was pumped through the lumen of the cryoloops, decreasing the cryoloop temperature. Once the cryoloop temperature was stable at 3 °C, we began the peri-cooling session. Cryoloop temperatures of 3 °C silence post-synaptic activity in tissue up to 1.5 mm away without influencing axonal propagation of action potentials (Lomber et al. 1999). Upon finishing the peri-cooling session, we turned off the cooling pumps, which allowed the cryoloop temperature to rapidly return to normal. When the cryoloop temperature reached 35 °C, we started the post-cooling session. Although saccadic behaviour and iSC activity rapidly recovered after rewarming, the post-cooling sessions may have contained residual effects of cooling. To minimize these and other time-dependent factors, we combined trials from pre- and post-cooling sessions into the *FEF warm* condition, which we compared to *FEF cool* condition (peri-cooling). We obtained similar results about the influence of FEF inactivation on iSC activity when only comparing the pre- and peri-cooling sessions.

2.2 Behavioural tasks

We recorded iSC activity while monkeys performed either immediate (direct, or gap) or delayed (visually, or memory-guided) saccade tasks (n.b., we did not record any iSC neurons with both delayed and immediate saccade tasks). In all tasks, the monkeys first had to look at a central fixation point, and hold fixation within a ± 3° window for a period of 750–1000 ms. On immediate saccade tasks, a peripheral cue was then presented either coincident with (direct saccade task) or 200 ms after (gap saccade task; central fixation was still required during this 200 ms gap) disappearance of the central fixation point. The monkeys then had 500 ms to look toward the peripheral cue within a spatial window (diameter set to 60% the visual eccentricity of the cue). The cue remained on for the direct saccade task, but was flashed for 150 ms in the gap saccade task. In the delayed saccade tasks, the central fixation point remained on following peripheral cue presentation for a fixed delay period of 1000 ms, during which the monkeys maintained central fixation. Peripheral cues were either extinguished after 250 ms (memory saccade task) or remained on for the remainder of the trial (delayed visually-guided saccade task). Monkeys had to saccade to the remembered (memory saccade task) or visible cue (delayed visually-guided saccade task) location (window diameter set to 70% the visual eccentricity of the cue) within 1000 ms after offset of the central fixation point, which served as the go-cue. Saccade onset and offset were determined using a velocity criterion of 30°/s. We excluded trials from our analysis where monkeys did not generate their first saccade towards the target, generated anticipatory saccades with saccadic reaction times <60 ms, or blinked during the trial.

For Experiment 1 where we characterized the effects of FEF inactivation on iSC activity at the center of neuron's response field, we usually recorded neurons with only one type of delayed saccade (*i.e.*, ~79% of iSC neurons were recorded with either memory or delayed visually-guided saccades), but we always recorded iSC neurons with both direct and gap saccades in an interleaved manner. Furthermore, we only recorded neurons with a single saccade task for Experiment 2 that sought to characterize the effects of FEF inactivation on neuronal response fields. Of the 28 isolated neurons that were studied in Experiment 2 and exhibited a clear response field, we recorded 8, 11, and 9 neurons with direct, delayed visually-guided, and memory-guided saccades

respectively. Given these small sample sizes and that FEF inactivation produced similar effects across tasks, we pooled results across saccade task in Experiment 2.

2.3 Neuron classification

In this study, we analyzed neurons exhibiting saccade-related activity. For classification purposes, we convolved individual spikes with a spike density function that mimics an excitatory post-synaptic potential (rise-time of 1 ms, decay-time of 20 ms, kernel window of 100 ms (Thompson et al. 1996)). To qualify as a saccade-related neuron, the mean peri-saccadic firing rates (defined in an interval spanning 8 ms before saccade onset to 8 ms prior to its end) had to be significantly greater than the last 100 ms before the go-cue ($p < 0.05$, Wilcoxon signed rank test), and the increase in peri-saccadic activity above baseline activity (last 200 ms before fixation cue offset in immediate response tasks, or last 200 ms before cue onset in delayed response tasks) had to exceed 50 spikes/s (McPeek and Keller 2002; Munoz and Wurtz 1995; Peel et al. 2017). Because the delayed saccade tasks allowed us to dissociate visual and saccade-related activity, we also differentiated visuomotor from motor neurons by looking for the presence or absence, respectively, of significantly increased visually-related activity (mean activity in a 50 ms window after the onset of any visually-related activity) compared to the last 200 ms before peripheral cue onset ($p < 0.05$, Wilcoxon signed rank test, see (Peel et al. 2017) for more details on quantification of visually-related activity). In addition, we carried out an analysis to determine the durations of saccade-related bursts across of sample of iSC neurons using a Poisson-detection method previously described in our earlier study (Peel et al. 2017). Note that saccade-related bursts usually ended subsequent to saccade offset across our sample of iSC neurons, but we measured the entire duration of the saccade-related burst for this analysis.

2.4 Dynamic linear ensemble-coding model

To explore the impact of FEF inactivation on iSC activity within the context of the dynamic linear ensemble-coding model (Goossens and Van Opstal 2006), we compared the cumulative number of saccade-related spikes for saccades of similar metrics within the four tasks we studied, with or without FEF inactivation. One prediction from the dynamic linear ensemble-coding model is that metrically-matched saccades should be associated with an equivalent number of spikes across the population of iSC neurons. Within a single neuron, we tallied the cumulative number of saccade-related spikes within a window spanning 20 ms before saccade onset to 20 ms before saccade offset (similar results were found if we used an interval shifted 8 ms relative to saccade onset and offset). The dynamic linear ensemble-coding model follows the framework of Eq. 1 whereby each spike ($k = 1, 2, \ldots, N$) from each iSC neuron ($i = 1, 2, \ldots, M$) adds a fixed site-specific amount ($\vec{e_i}$) convolved with a delta function (δ) to the saccade vector following a delay (τ):

$$\Delta\vec{E}(t) = \sum_{i=1}^{M} \sum_{k=1}^{N_i(t)} \vec{e_i} \cdot \delta\,(t-\tau) \tag{1}$$

In an implementation of the model described previously (see Fig. 6 of Goossens and Van Opstal 2006), the brainstem circuits below the iSC simply read out spatial activity for horizontal and vertical components in two independent linear feedback systems; normal saccade dynamics can be realized after optimizing five fixed parameters (γ_h and γ_v, respective scaling factors for each horizontal and vertical component based on projection strength, B, feedforward gain of saccade burst neurons, and τ and d, fixed delays of brainstem activation and of the feedback loops, respectively; see also Fig. 7a). Interestingly, more recent studies implementing this model (Van der Willigen et al. 2011) have found that only two free parameters, the feedforward gain of the burst generator and the delay of brainstem activation, were sufficient to create realistic saccades.

We also constructed saccades from measured iSC activity using the dynamic linear ensemble-coding model, albeit using a slightly modified approach from (Goossens and Van Opstal 2006). Specifically, we retained the framework and all parameters from the model (*i.e.*, γ_h, γ_v, B, τ, and d), but we measured iSC activity with and without FEF inactivation from paired trials having displacement-matched saccades for each task condition (see below for matched saccade procedure). While examining all iSC responses to the same saccade vector would be more reflective of the original model, our limited dataset of iSC response fields from Experiment 2 meant that our only practical implementation of the model was to use those iSC neurons obtained from Experiment 1. While we acknowledge that our implementation of the model is a simplification, this approach could provide novel insights into how the readout of iSC activity in the brainstem changes with FEF inactivation.

To estimate iSC activity over time for the purpose of reconstructing saccades using this model, we followed a similar procedure from (Goossens and Van Opstal 2006). Namely, we mapped spikes from each neuron on a 2D anatomical map of the iSC (spatial and temporal resolution of 0.1 mm and 1 ms, respectively), and then used a gaussian function centered at each location [x_i,y_i] and having a width of 0.1 mm (ω) to spatially smooth data at each timepoint. We estimated iSC activity at each coordinate, f(t), using Eq. 2, where $S_i(t)$ represents the recorded spike events of neuron i out of M total number of neurons.

$$f(t) = \sum_{i=1}^{M} S_i(t) exp\left[-\frac{(x-x_i)^2 + (y-y_i)^2}{2\omega^2}\right] \tag{2}$$

The mini-vector contribution of each iSC spike used in the dynamic linear ensemble-coding model (*i.e.*, $\overrightarrow{e_i}$ of Eq. 1) depended upon the site-specific connection strengths with the brainstem, which is based on prior neurophysiology evidence (Moschovakis et al. 1998). Hence, we calculated the corresponding mini-vectors used in the horizontal and vertical premotor systems by multiplying each iSC spike by a fixed scaling parameter (γ_h and γ_v, respectively) and the standard efferent mapping function (Van Opstal and Van Gisbergen 1989). We then estimated the horizontal and vertical eye velocity signals by linear summation of all mini-vectors from all iSC cells according to Eq. 1 (2 ms resolution, and a iSC to brainstem delay of τ ms). Each of the horizontal vertical premotor systems operated in linear feedback loops (see Fig. 7A or Fig. 6 of Goossens and Van Opstal 2006), such that the integrated sum of mini-vectors (minus the feedback following a delay of d) was multiplied by a feedforward gain (B) to invigorate the burst cells within each of the horizontal and vertical premotor areas. This burst provided an estimate of displacement or feedback that was used in the prior integration stage, and also innervated the motoneurons (using a pulse-step signal) that moved the eyes with a 1st-order eye plant ($\frac{1}{1+sT}$, where T is a time constant of 150 ms, and 1/s represents neuronal integration using Laplace notation).

We estimated r^2 values, or the ability of the model to explain saccade trajectories using iSC activity, by fitting the reconstructed horizontal and vertical eye traces to the actual traces (both displacement and velocity). To obtain parameter values (γ_h, γ_v, B) for each of the FEF warm and cool conditions, we ran a nonlinear optimization algorithm (Nelder-Mead simplex method, (Goossens and Van Opstal 2006)) to minimize residuals. We repeated this procedure for each combination of discrete time variables (τ and d), and chose values based on highest r^2 values obtained across FEF warm and cool fits. We also tested how an individual parameter could explain FEF cool data, whereby we reran the optimization algorithm with fixed FEF warm values and only allowing one or two parameters to vary.

Finally, in order to speculate on alternate neuron mechanisms of how FEF inactivation alters the readout of iSC activity, we also explored a modified implementation of the dynamic linear ensemble-coding model that partly accounts for cerebellum-brainstem circuitry. Specifically, as shown in Fig. 8a, we mostly retained the main iSC pathway to the horizontal and vertical premotor systems, but we removed the linear feedback and made the vector summation mechanism "leaky". Namely, instead of complete integration of iSC inputs where there exists little supporting neurophysiology evidence (see Smalianchuk et al. 2018), we convolved velocity signals arising from the iSC with a spike-density function that mimics an excitatory postsynaptic potential (rise time of 1 ms and decay time of 20 ms, kernel window of 100 ms; (Thompson et al. 1996)). Moreover, we added a new pathway from the iSC to each horizontal and vertical premotor system *via* a cross-coupled pathway *via* the cerebellum (*i.e.*, is not spatially encoded, and only provides a gain signal). We surmised that the midbrain NRTP could integrate iSC signals minus those arising from the neuronal integrators in each of the horizontal (PrH, nucleus prepositus hypoglossus) and vertical (NIC, interstitial nucleus of Cajal) premotor systems, and relay this signal to the cFN (caudal fastigial nucleus) *via* the OMV (oculomotor vermis, ε in the modified model). The cFN could then provide a linear gain signal to both the horizontal and vertical premotor system (cFN = αNRTP + ε, where α is constant and equal to 1 in the FEF warm condition). We tested if varying this gain from the cFN (α and ε) could provide valid fits to FEF cool data without the need to change any additional parameters.

2.5 Matched-saccade procedure

FEF inactivation increases the RT and decreases the accuracy and velocity of contralateral saccades (Peel et al. 2014). Even with such changes, there were overlapping distributions of saccade vectors with or without FEF inactivation, and we exploited this overlap in the current study. As described below, one of the means by which we test the model across FEF inactivation is to find instances where a very similar saccade is generated with or without FEF inactivation, while the same neuron was being recorded. To compare cumulative spike counts of such metrically-matched saccades, we first ranked each FEF cool trial with FEF warm trials based on the difference in horizontal and vertical displacement. We then matched without replacement each FEF cool trial with the FEF warm trial that contained the lowest combined rankings (we used a similar matching procedure in our previous study (Peel et al. 2017), modifying it here to not include previously matched trials and to be agnostic of differences in peak velocity). We specified that any such matched saccades had to have differences of horizontal and vertical displacements less than 1.5°, but matches usually had differences in horizontal and vertical displacements much less than 1° (mean ± SD of 0.002 ± 0.235° and − 0.017 ± 0.280° across 4449 matched pairs of trials with ipsilesional iSC recordings, respectively). In some analyses, we also tested whether this matching procedure biased any results by performing a similar matching procedure utilizing only FEF warm trials. To do this, we matched each FEF warm trial to a different FEF warm trial that had the lowest ranked differences in horizontal and vertical saccade displacements.

2.6 iSC representations of population activity and its influence on saccade displacement

The dynamic linear ensemble-coding model posits each saccade-related spike from the population of active iSC neurons adds a fixed, site-specific displacement vector to the saccade trajectory; in doing so, the model makes no assumptions

about the spatial distribution of saccade-related activity throughout the iSC. In other words, all iSC neurons in the population, regardless of location, can influence a given saccade trajectory. Hence, if FEF inactivation caused any changes in spike counts at the center of a given neuron's response field (which we test in Experiment 1), then such differences could be readily accounted for in the model by coincident changes that maintain a fixed total spike count across the population.

One potential confound is that the tuning curve of iSC response fields changes during FEF inactivation, whereby the response field could expand (fires more) or shrink (fires less) for off-center saccades. From the additional 28 isolated iSC neurons recorded for Experiment 2, we examined the influence of FEF inactivation on saccade-related response fields. To do this, we first constructed separate response fields for neural activity recorded during saccades generated with or without FEF inactivation. We then found the average spike count for each point ±2° within a 2D grid of saccade displacement (spacing of 1°), normalizing data based on the FEF warm condition (subtracting minimum value and then dividing by max value), and then linearly interpolating data to create a 2D colourmap. We then identified various contour levels of spike counts (0.3, 0.5, 0.7, and 0.9; 1.0 represents peak spike count from the FEF warm condition) in each of the FEF warm and cool conditions, which provided a comparative measure for how FEF inactivation influenced the center and tuning width of a neuron's response field.

To better quantify changes in spike counts during FEF inactivation, we also employed a static response field model of Ottes et al. (1986), which is illustrated by Eq. 3.

$$N = N_s \cdot exp\left[-\frac{(x-x_c)^2 + (y-y_c)^2}{2\sigma^2}\right] \quad (3)$$

Parameter N_s represents the maximal spike count in the response field, which is located at x_c and y_c within the iSC map (center position defined in mm). The decay rate or tuning width of the response field is governed by σ (also defined in mm and corresponding to the radial distance from the response field center to ~61% of peak response). For each neuron and cooling condition, we identified the values of four parameters (N_s, x_c, y_c, and σ) that satisfied the least squares criterion using a nonlinear optimization algorithm (Goossens and Van Opstal 2006). Of the 28 saccade-related response fields tested in this manner, we only excluded 4 iSC neurons for further analyses that did not produce reasonable estimates of the maximal spike count parameter (N_s between 5 and 50 spikes in the FEF warm condition). Importantly, this static field model of response fields obtained robust fits to FEF warm data (Pearson's correlation ranged between 0.55 and 0.87 across our sample of 24 neurons), which did not significantly change with FEF inactivation ($p = 0.42$, $z = -0.8000$, Wilcoxon signed rank test). Average parameter values ± standard deviation for N_s, x_c, y_c, and σ in the FEF warm condition were 12 ± 6 spikes, 2.7 ± 1.2 mm, 0.2 ± 0.8 mm, and 0.9 ± 0.3, respectively. While our average spike counts and tuning widths are different compared to values (N_s = 20 ± 9 spikes, σ = 0.5 ± 0.2 mm) reported by (Goossens and Van Opstal 2006), such differences may relate to the reduced vigor of iSC activity in the delayed saccade tasks compared to immediate saccade tasks employed in the earlier study by Goossens and Van Opstal (2006). Finally, because changes in these parameters may covary with FEF inactivation, we also tested whether FEF inactivation induced any expansion or shrinkage of response field width (σ). To test this, we performed a second fitting procedure on the FEF cool data using fixed parameters of N_s, x_c, and y_c extracted from the FEF warm fit, and only allowed the remaining σ parameter to vary.

A central assumption of the model is that the total number of spikes emitted from the iSC monotonically increases along the saccade trajectory to a fixed boundary. Thus, if the population output is changing, then this change should be reflected in the relationship between instantaneous saccade displacement and the cumulative spike count across our neuron sample, which does not require any matching procedure. For this analysis, we used those iSC neurons collected in Experiment 1 and regressed a linear relationship to each neuron, such that the slope indicates the cumulative spike count per unit of displacement (again with an offset of 20 ms). We then computed the average intercept and slope value across our neuron sample in each task, with and without FEF inactivation.

2.7 Experimental design and statistical analysis

Our analysis of the effects of FEF inactivation on iSC activity exploits the overlap of saccade vectors with and without FEF inactivation, such that we could examine differences in iSC activity between matched trials having similar saccade vectors towards the center of the response field. To quantify the effects of FEF inactivation on saccadic behaviour and related measures of iSC activity, we usually performed paired Wilcoxon singed-rank tests to find statistical differences within individual neurons and across the neuronal population at $p < 0.05$. We also investigated how FEF inactivation influenced the response fields of iSC neurons by comparing parameters generated from a response field model (Ottes et al. 1986) with and without FEF inactivation. We used paired Wilcoxon singed-rank tests to uncover statistical differences across individual iSC neurons and across the neuronal population at $p < 0.05$.

3 Results

In this study, we tested if the dynamic linear ensemble-coding model proposed by (Goossens and Van Opstal 2006) is robust

to FEF inactivation across four saccade tasks (direct, gap, delayed visually-, and memory-guided saccades). In experiment 1, we focus on activity recorded from 150 saccade-related iSC neurons (83 from Monkey DZ, and 67 from Monkey OZ) recorded ipsilateral to the side of FEF inactivation while monkeys performed saccades towards peripheral cues placed at the center of a neuron's response field. Although FEF inactivation produced a triad of saccadic deficits for contralaterally-directed saccades (reduced accuracy, and peak velocities, and increased reaction times) in every task, a substantial overlap of saccade metrics allowed us to test the model for saccades matched closely for saccade metrics. Indeed, our matching procedure without replacement matched 93% of FEF cool trials with a FEF warm trial containing very similar saccade metrics (see **Methods** for details). We first demonstrate how FEF inactivation influenced spike counts in an exemplar iSC neuron for matched saccades in a single task, then we characterize the effects of FEF inactivation across the sample of recorded iSC neurons, and across different saccade tasks. In experiment 2, using data from an additional 28 iSC neurons recorded ipsilateral to FEF inactivation, we examined the impact of FEF inactivation on neurons' movement fields within the context of the model. Finally, we examine which model parameters that influence the brainstem readout of iSC activity could explain the effects of FEF inactivation on saccade dynamics.

3.1 FEF inactivation reduced cumulative spike counts in iSC neurons for displacement-matched saccades

In contrast to what would have been predicted by the model if it were to operate independently of any supra-tectal inputs, FEF inactivation reduced the cumulative spike counts for saccades of matched displacement. Figure 1a shows data for a pair of matched saccades from the delayed visually-guided saccade paradigm. These saccades were closely matched for horizontal and vertical displacement (displacement differences less than 0.1° for FEF warm and cool conditions). As expected, FEF inactivation decreased peak saccade velocity (from 709 to 527 °/s in this case) and increased saccade duration (from 49 to 53 ms). Despite the similarity in saccade metrics, FEF inactivation markedly reduced the cumulative spike count from 24 to 12 spikes during the interval spanning from 20 ms before saccade onset to 20 ms before saccade offset (see shaded area with spike trains in Fig. 1a).

We repeated this procedure for all trials recorded from this neuron, matching saccades generated in the FEF cool condition to one generated in the FEF warm condition; doing so yielded 23 matched pairs. The mean (± SE) displacement and radial velocity of these matched pairs is shown in the inset of Fig. 1b, emphasizing the close match in saccade displacement despite decreases in saccade velocity and corresponding increases in saccade duration. Across all matched trials recorded from this iSC neuron (plotted in order in the rasters of Fig. 1b), we observed a significant decrease in the cumulative number of spikes from 16 to 10 in the FEF warm to cool conditions ($p < 10^{-5}$, $z = 4.4211$, Wilcoxon signed-rank test), despite a significant increase in saccade duration from 48 to 65 ms ($p < 0.0001$, $z = -4.2002$, Wilcoxon signed-rank test). Hence, despite increases in saccade duration and the generation of metrically-matched saccades, the total number of saccade-related spikes emitted by this iSC neuron decreased during FEF inactivation.

3.2 Cumulative spike counts for metrically-matched saccades decreased during FEF inactivation in a task-dependent manner

The neuron shown in Fig. 1b exhibited one of the larger changes in cumulative spike count during FEF inactivation. Across the sample of recorded neurons, FEF inactivation reduced cumulative spike count during the saccade interval, with larger reductions in spike count accompanying saccades generated during more cognitively demanding saccade tasks. Of the four saccade tasks, FEF inactivation caused the largest reductions in the cumulative spike count during memory-guided saccades (black dots in Fig. 2a; cumulative spike count decreased by 10% across 58 iSC neurons; $p < 0.001$, $z = 3.6428$, Wilcoxon signed-rank test), and the next largest reductions during delayed visually-guided saccades (grey dots in Fig. 2a; cumulative spike count decreased by 6% across 62 iSC neurons; $p < 0.01$, $z = 3.0922$, Wilcoxon signed-rank test). Since these tasks dissociate visual and saccade-related activity, we investigated whether the reduction in cumulative spike count during FEF inactivation related to the cell's functional classification. Although FEF inactivation produced larger decreases of cumulative spike counts in pure motor neurons compared to visuomotor neurons, these spike count differences between neuron classifications did not significantly differ in the memory- ($p = 0.62$, $z = -0.4935$, Wilcoxon rank sum test) or delayed visually-guided saccade tasks ($p = 0.82$, $z = -0.2296$, Wilcoxon rank sum test). Again, FEF inactivation reduced cumulative spike counts across iSC neurons even though saccade durations increased, which change was reflected in the increased durations of saccade-related bursts of matched memory- (157 to 166 ms, $p < 0.05$, $z = -2.3343$, Wilcoxon signed-rank test) and delayed visually-guided saccades (92 to 105 ms, $p < 0.0001$, $z = -4.7851$, Wilcoxon signed-rank test).

Compared to the results in the delayed saccade tasks, FEF inactivation decreased cumulative spike counts in the gap and direct saccade tasks by a smaller amount of 4 and 2%, respectively, and these effects did not reach significance across our sample (Fig. 2b, both 43 neurons, $p = 0.15$ and 0.11, $z = -1.4407$ and -1.5808, respectively, Wilcoxon signed-rank tests).

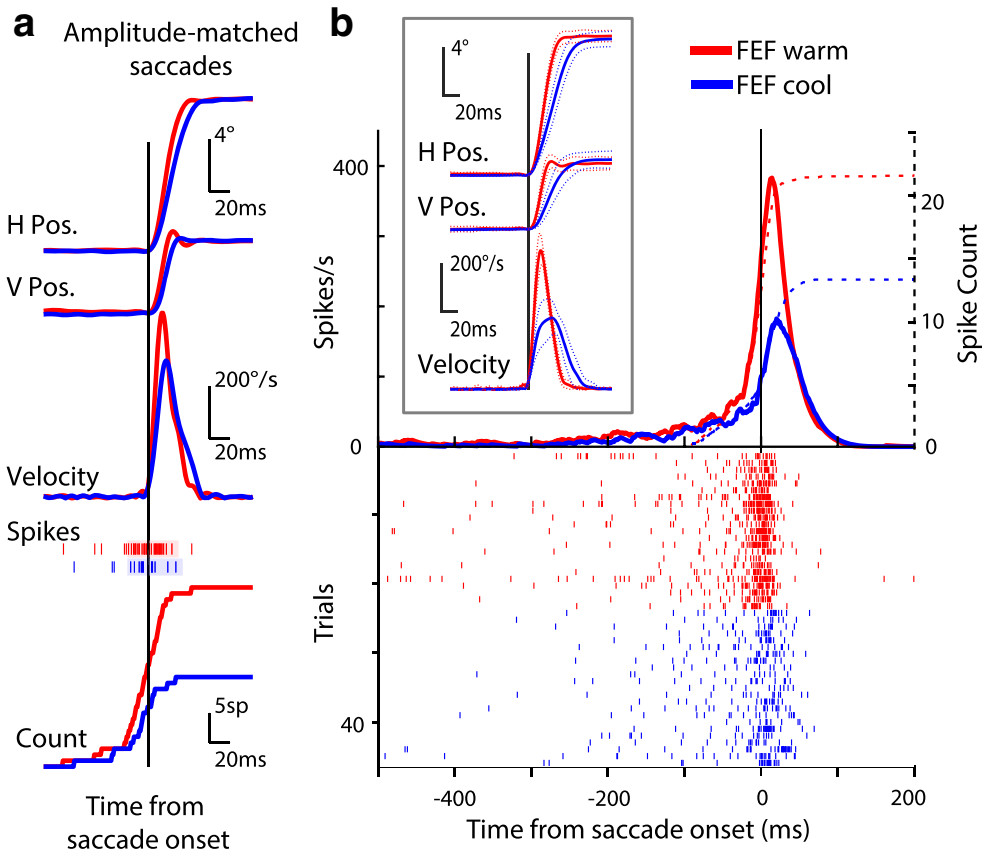

Fig. 1 FEF inactivation reduces the cumulative spike counts in iSC neurons for metrically-matched saccades. (**a**) Spike rasters and cumulative density functions (CDF) from one matched pair of delayed visually-guided saccades. Our matched saccade analysis compared saccades of very similar eye position profiles but different kinematics and reaction times across FEF warm or FEF cool conditions. Shaded region within spike train indicates period between saccade onset to offset. (**b**) Spike rasters (below) and mean spike density functions (above) showing reduced cumulative spike counts in an example ipsilesional iSC neuron during FEF inactivation. Note how metrically-matched, delayed visually-guided saccades had reduced peak velocities, and longer durations with FEF inactivation (inset). Spike count indicates the cumulative number of spikes starting 100 ms before saccade onset

The impact of task is summarized in Fig. 2c (blue bars), emphasizing how FEF inactivation produced larger and more consistent reductions of cumulative spike count for saccade tasks with increasing cognitive demands (*i.e.* delaying response, and remembering peripheral cue location). As a control, we repeated our matching procedure using data only from FEF warm trials (*i.e.*, a given FEF warm trial would be paired with a different FEF warm trial of closely matched displacements); doing so reveals the amount of noise inherent to the matching procedure. Across all four saccade tasks, cumulative spike counts did not change (all differences less than 1.1%, $p > 0.30$, Wilcoxon signed-rank tests) when FEF warm trials were matched to other FEF warm trials (red bars and symbols, Fig. 2c).

The above analysis averages the number of saccade-related spikes within a given neuron for qualifying matched saccades, and then plots the change across FEF inactivation on a neuron-by-neuron basis. We also performed an analysis where each matched pair was treated as its own sample; doing so gives a sense of the trial-by-trial variability inherent to FEF inactivation, and to the matching procedure. The results of this analysis are shown in Fig. 3a for the memory-guided saccade task. Here, the size of each square is proportional to the number of trials with the observed number of spikes across matched pairs; for example, the square indicated by the grey arrow shows 9 matched trials (across all of our sample) that had cumulative spike counts of 9 and 4 spikes in the FEF warm and FEF cool condition, respectively. While this analysis shows considerable variation around the line of unity, FEF inactivation shifted the cumulative spike counts towards reduced values (blue histograms, 9% decrease, $p < 10^{-15}$, $z = 8.1776$, number of matched trials = 1027, Wilcoxon signed-rank test). In contrast, we observed negligible shifts when we matched only FEF warm trials in the memory-guided saccade task (red histograms in Fig. 3a, $p = 0.60$, $z = -0.5253$, matched pairs = 1624, Wilcoxon signed-rank test).

When analysed this way, we observed significant reductions in cumulative spike counts in all four tasks when FEF warm and FEF cool trials were matched (blue symbols and lines in Fig. 3b), but not when FEF warm trials were matched to FEF warm trials (red symbols and lines in Fig. 3b). As before, the magnitude of reduction varied with the saccade task, with the largest decreases accompanying saccades generated in the memory-guided saccade task (−9%), then the delay task (−8%, $p < 10^{-11}$, $z = 7.0282$, Wilcoxon signed-rank test), then the gap task (−6%, $p < 0.01$, $z = -2.8047$, Wilcoxon signed-rank test), and finally the direct-saccade task −4%, $p < 0.05$, $z = -2.1082$, Wilcoxon signed-rank test). Recall that the cue was flashed for only 150 ms for gap but not direct saccades, hence saccades in the gap saccade task did not always land on a visible target (~54% of gap saccades had RTs greater than 150 ms without FEF inactivation).

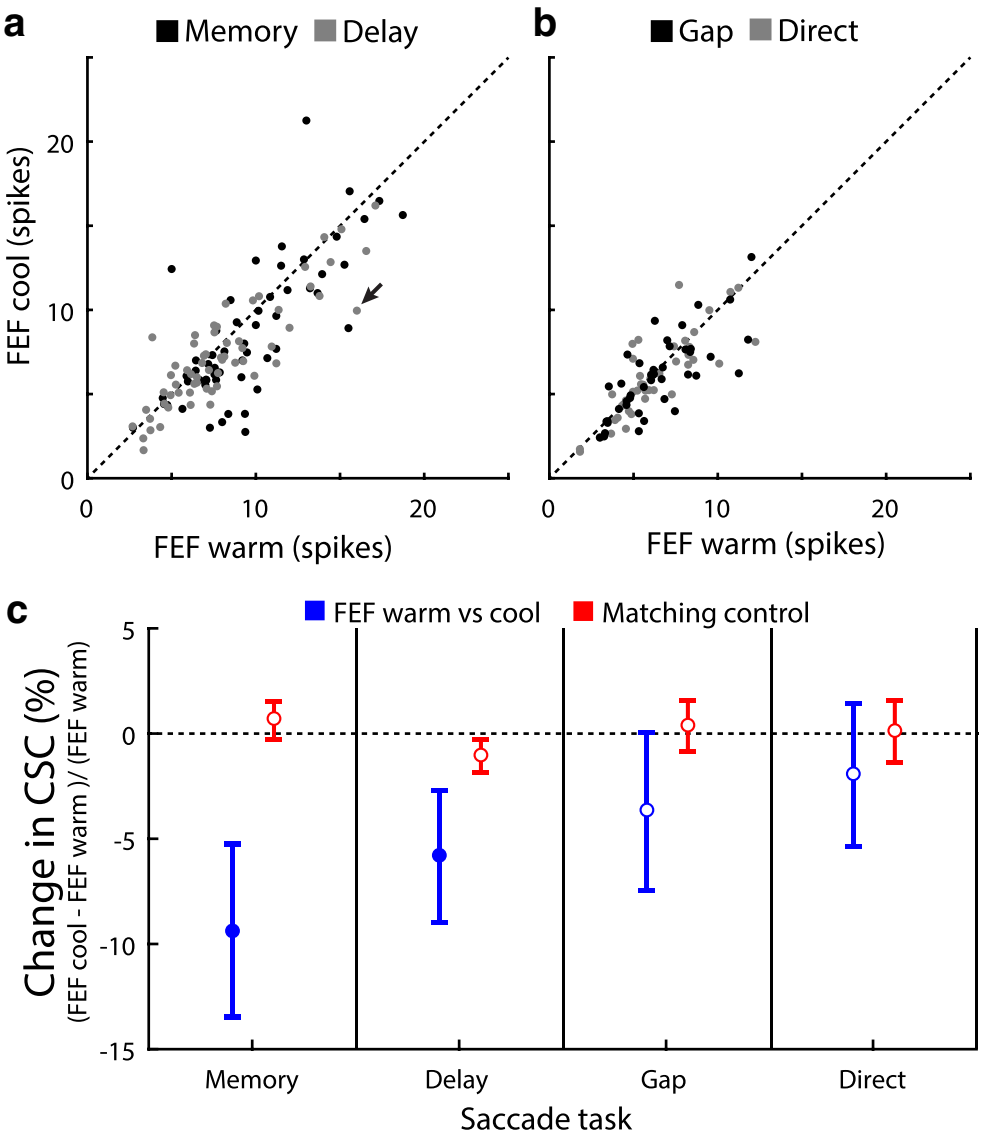

Fig. 2 The reduction in iSC spike count during FEF inactivation scaled with task demands. (**a**) FEF inactivation consistently decreased the cumulative number of spikes during saccades (20 ms before saccade onset to 20 ms before saccade offset) across the population of ipsilesional iSC neurons for both memory- and delayed visually-guided saccades. (**b**) FEF inactivation often reduced the cumulative spike count during gap and direct saccades, but these decreases were not consistent across the population of iSC neurons. (**c**) FEF inactivation caused greater and more consistent decreases of cumulative spike count depending upon the saccade task (blue lines, mean ± SE). Such inactivation effects were most commonly observed for memory saccades followed by delayed visually-guided, gap, and finally, direct saccades, but did not occur with a similar matching procedure of only FEF warm trials (red lines). Filled circles indicate significant results at 0.05 criterions

Collectively, the results in Figs. 2 and 3 show that FEF inactivation decreased the cumulative number of spikes in ipsilesional iSC neurons for displacement-matched saccades in a task dependent manner. Next, we evaluated whether spike-count reductions in the ipsilesional iSC during FEF inactivation could be related to changes in fixation position.

3.3 Differences in fixation position cannot explain cumulative spike count decreases during FEF inactivation

FEF inactivation produces slight deviation in fixation position towards the intact side (see Fig. S1 of Peel et al. 2016). Could the reduction in spike count for displacement-matched saccades be related to such changes in fixation position? To explore this question, we divided matched pairs of trials into two subsets using a median-split procedure of fixation error when the FEF was inactivated (see Fig. 4a for the segregation of high and low fixation errors at saccade onset for FEF cool trials). Doing so created one subset of FEF warm trials matched to FEF cool trials with a larger-than-average fixation error, and another subset of FEF warm trials matched to FEF cool trials with a smaller-than-average fixation error. As expected, the fixation error for the higher-than-average subgroup was significantly greater during FEF cool *versus* FEF warm trials (increase of 0.5271°, $p < 10^{-35}$, $z = 12.5138$, Wilcoxon sign-rank test). Critically, the fixation error for the lower-than-average subset was significantly *less* during FEF cool *versus* FEF warm trials (decrease of 0.2274°, $p < 10^{-7}$, $z = -5.3877$, Wilcoxon sign-rank test). We then analyzed the reductions in spike count for these two subsets, and found that cumulative spike count in the SC decreased to the same degree during FEF inactivation, regardless of the magnitude of any fixation error (Fig. 4b and c show that spike count decreased by 10 or

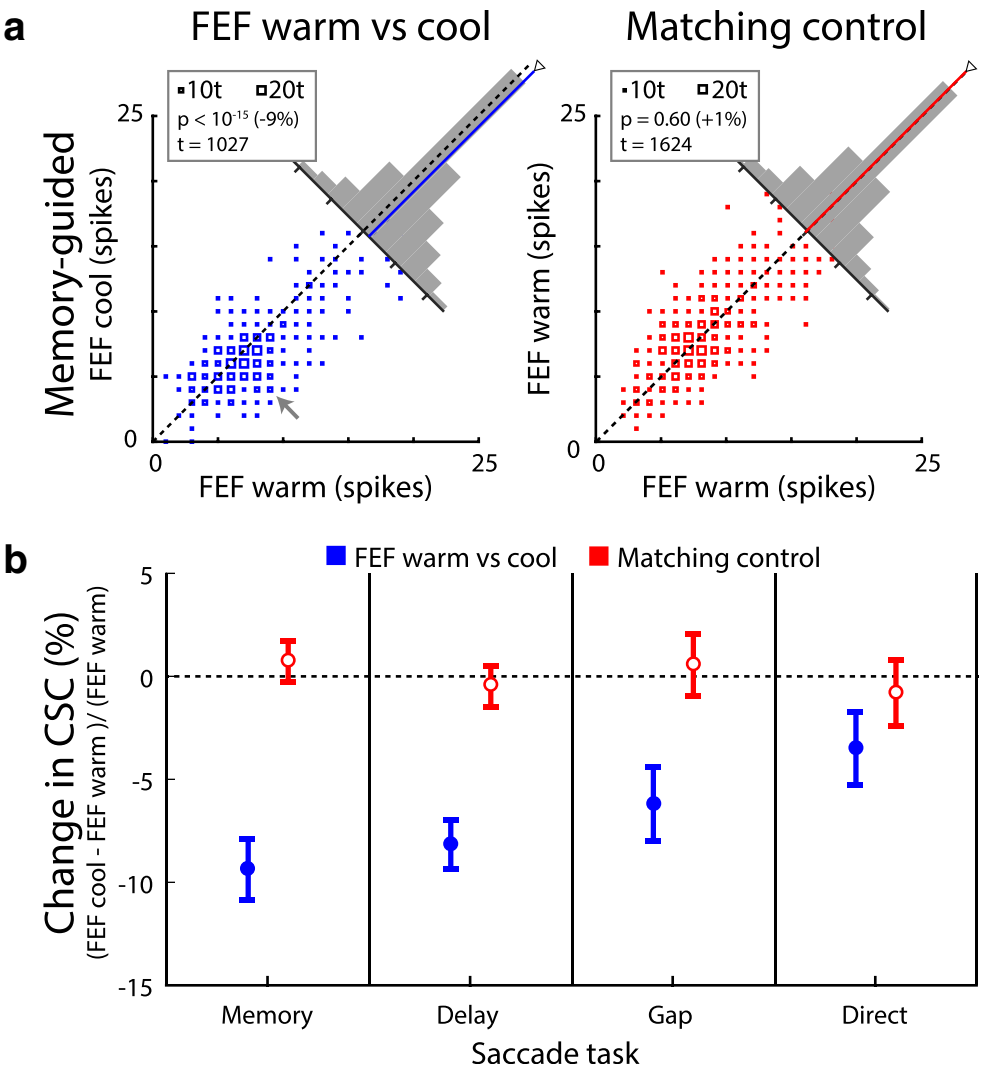

Fig. 3 A trial-by-trial analysis of iSC spike counts revealed reductions during FEF inactivation across all tasks. (**a**) As shown for the memory-guided saccade task, FEF inactivation reduced cumulative spike counts across trials matched for saccade metrics (blue bars). Note how histograms are skewed towards decreased cumulative spike counts. In contrast, we found invariant cumulative spikes when matching only FEF warm trials (red bars). Each square represents the occurrence of a given pairing of spike counts, with number of occurrences of a particular pairing represented as the size of the square (see insert for reference). (**b**) Across trials, FEF inactivation produced larger relative reductions in cumulative spike count depending upon saccade task (mean ± SE). Same format as Fig. 2c

9% for the greater-than-average or lower-than-average FEF cool fixation error in the memory-guided saccade task, respectively; $p < 10^{-7}$ Wilcoxon signed-rank test for both subgroups, $z = 6.2382$ and 5.3914, respectively). We found a similar lack of effect of fixation error for all saccade types, and for different measures of fixation error (*e.g.*, averaged during the entire pre-cue period, or when the horizontal or vertical component of fixation error was analyzed separately; data not shown). Overall, these analyses emphasize that changes in fixation error cannot explain the reductions in cumulative spike count in the SC during FEF inactivation.

3.4 FEF inactivation reduces the cumulative number of saccade-related spikes throughout the response field

Up to now, our analyses have focused on matched saccades generated toward cues placed at the estimated center of a neuron's response field. However, the dynamic linear ensemble-coding model of Goossens and Van Opstal (2006) is based on the population of spike activity across all iSC neurons active for a given saccade. Could decreases in spike count during FEF inactivation be explained by increased spike counts across a neurons' response field to produce the same saccade? If so, we would expect the decreases in spike count from the center of the response field be compensated by spike count increases at off-center locations, which correspond to shifts or expansion of the response field's tuning curve. To explore these possibilities, we analyzed data in experiment 2 where we characterized the entire saccade-related response field with and without FEF inactivation.

We constructed saccade-related response fields (see **Methods** for more details) with and without FEF activation, normalizing all data to the peak of the FEF warm response field for analysis across our sample. We then compared a number of parameters of the response field across FEF inactivation. An example of the saccade-related response fields from a representative neuron recorded with or without FEF inactivation is shown in Fig. 5a**.** In this example, and consistent with our previous results, we found

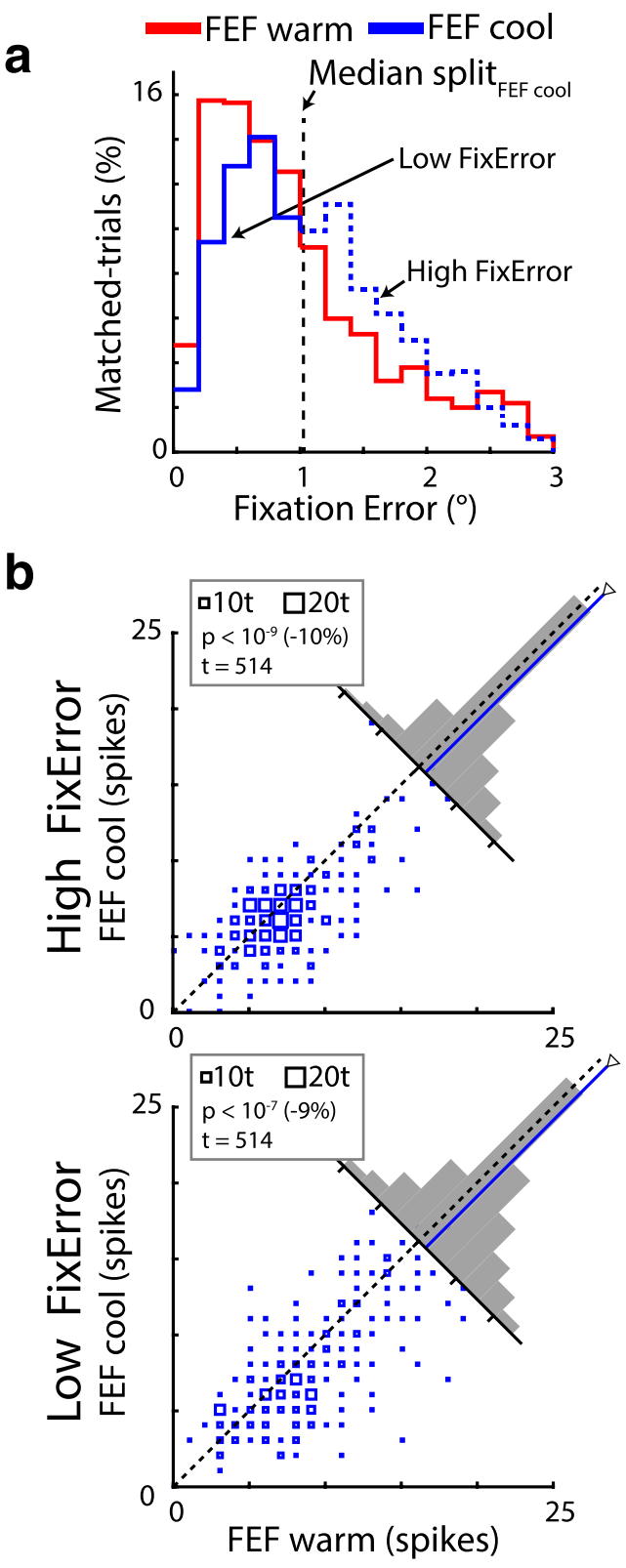

Fig. 4 FEF inactivation reduces iSC spike counts for metrically-matched saccades regardless of fixation position. (**a**) As shown across all matched trials in the memory-guided saccade task, FEF inactivation (trials represented in blue) skewed the distribution of radial position error at the start of the saccade towards larger errors (compare to FEF warm trials represented in red). The blue vertical line represents the median value from FEF cool trials, which we used for the median-split analysis. (**b**) For both subsets of matched trials containing either high (top) or low (bottom) fixation error values in this task, FEF inactivation reduced cumulative spike counts as shown by the rightward skewness in the histograms. Same format as Fig. 3a, separated into subsets with higher- or lower- than average fixation error

that FEF inactivation decreased the peak cumulative spike count during the saccadic interval for movements to the center of the response field (from 10 to 7 spikes), and other measures of peak saccade-related activity (in this case, 200 to 132 spikes/s). Moreover, the various contour levels (0.3 to 0.9 in 0.1 increments) reveals that FEF inactivation did not drastically alter the shape or extent of the movement field of this iSC neuron.

To quantify these effects across our sample, we employed a nonlinear optimization algorithm on a static response field model of Ottes et al. (1986) to obtain parameters that characterized key aspects of the response field (peak spike count, N_s; tuning width, σ; horizontal and vertical center position in SC, x_c and y_c, respectively, see **Methods** for details). The results from this analysis on the same neuron are shown in Fig. 5b which again shows how FEF inactivation blunted the peak spike count (10 to 8 spikes) at the response field center without affecting this position within the SC map (horizontal and vertical differences less than 0.2 mm). While FEF inactivation slightly increased the tuning width from 0.46 to 0.54 mm, such increases may be due to coincident changes in the other three parameters. Specifically, in a second fit of FEF cool data where we fixed the N_s, x_c and y_c parameters based on FEF warm data (hence only σ could vary), we in fact found a smaller tuning width during FEF inactivation (0.45 mm). This illustrates how FEF inactivation primarily blunted the peak spike count of iSC response fields without systematically changing its tuning width, suggesting that the overall spike count from this neuron decreased regardless of saccade vector.

Across 24 of 28 isolated iSC neurons that had reasonable estimates of peak spike count in the FEF warm data (N_s between 5 and 50 spikes), the response field model provided robust fits that did not decrease with FEF inactivation nor with the three saccade tasks utilized (Fig. 5c, and see **Methods**), hence we first compare results pooled across tasks than individually (7, 10, and 7 neurons for the memory, delayed visually-guided, and direct saccade tasks, respectively). Compared to the exemplar iSC response field, we found similar changes to parameters with FEF inactivation (Fig. 5D). FEF inactivation significantly reduced the peak spike count across our sample from 12 to 10 ($p < 0.01$, $z = 3.2286$, Wilcoxon signed-rank test), but had no overall effect on tuning widths (0.89 to 0.87 mm, $p = 0.98$,

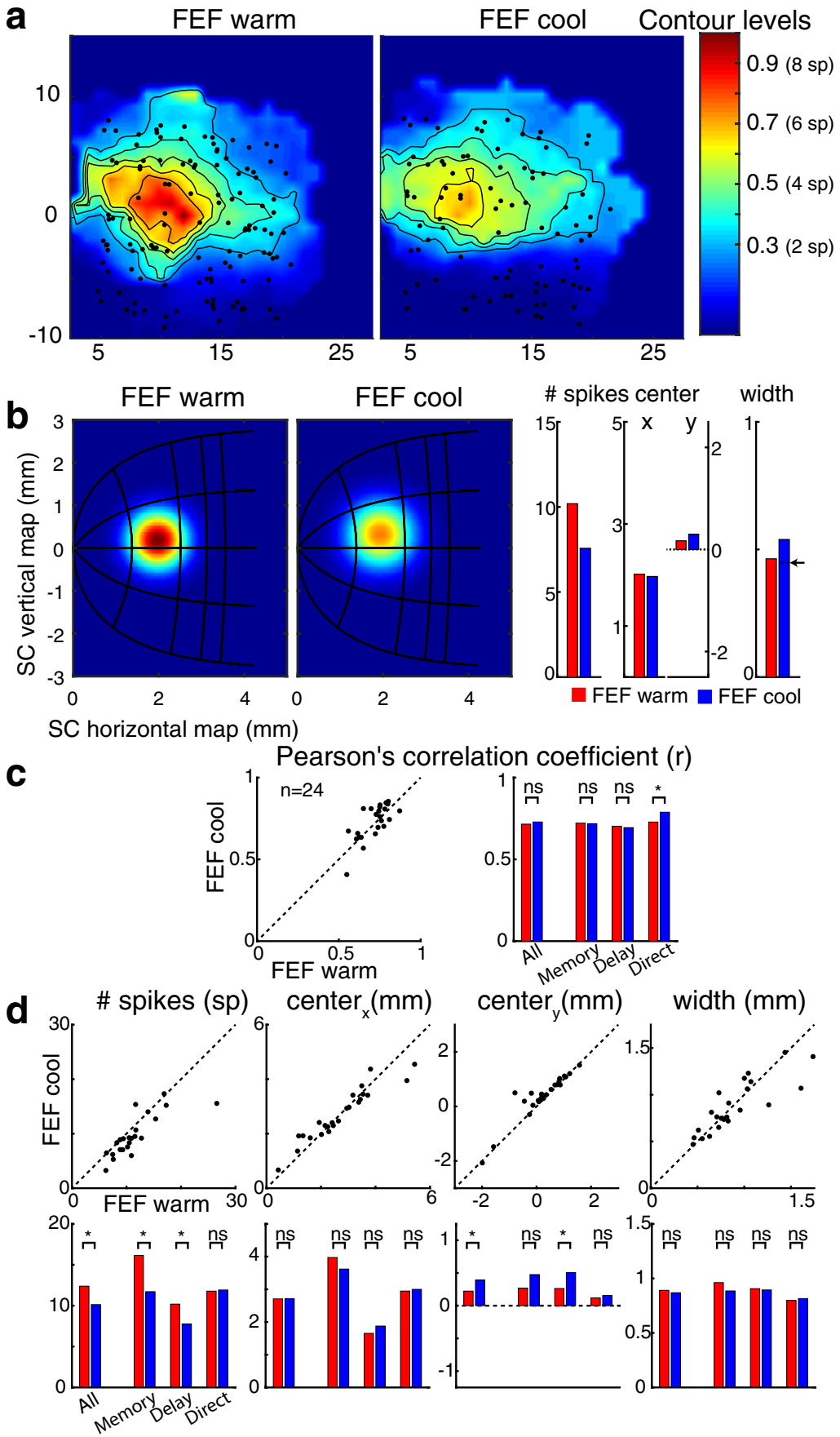
a
FEF warm
FEF cool
Contour levels
0.9 (8 sp)
0.7 (6 sp)
0.5 (4 sp)
0.3 (2 sp)
b
FEF warm
FEF cool
spikes center
width
SC vertical map (mm)
SC horizontal map (mm)
x
y
FEF warm
FEF cool
c
Pearson's correlation coefficient (r)
n=24
FEF cool
FEF warm
ns
*
All
Memory
Delay
Direct
d
spikes (sp)
center$_x$(mm)
center$_y$(mm)
width (mm)
FEF cool
FEF warm
All
Memory
Delay
Direct

◀ **Fig. 5** FEF inactivation reduces the overall spike count of iSC neuron population. (**a**) As shown for an example iSC neuron, FEF inactivation decreased spike count across its entire response field. As further detailed in the **Methods**, we characterized response fields two ways. Firstly, we performed a linear interpolation procedure of spike counts for each measured saccade displacement, where data within each plot is normalized to the maximum spike count in the FEF warm condition (value of 1). Shrinking of fixed contour lines with FEF inactivation reveal a blunting of spike counts at the center of the neuron's response field. (**b**) Secondly, we employed a static response field model to quantify changes in this example neuron, whereby we used a least squares criterion within a nonlinear optimization algorithm to search for four key parameters (peak spike count, horizontal and vertical position in SC map, and tuning width) characterizing response fields in each cooling condition. Note that we used a standard representation of visual space within the iSC as implemented within the model, but this is likely an over-simplification for the upper and lower visual field (Hafed and Chen 2016). In this example neuron, FEF inactivation reduced the peak spike count with only modest differences in other model parameters. An additional fit of FEF cool data using parameter values extracted from fits to the FEF warm condition except for tuning width revealed a negligible influence of FEF inactivation on tuning width (compare red bar with value indicated by arrow). This is consistent with the modest changes in tuning width during FEF inactivation being due to coincident changes in other parameters, including the blunting of the peak spike count. (**c**) Across our sample of 24 iSC neurons, Pearson correlation coefficients above 0.7 for the employed the response field model illustrate its robust fitting of the data, regardless of FEF inactivation and saccade task. Asterisks indicate significant differences with FEF inactivation having p values less than 0.05 in Wilcoxon signed-rank tests. (**D**) FEF inactivation consistently reduced the peak spike count across our sample (except for direct visually-guided saccades), with modest effects to the vertical position of response fields within the SC map. Importantly, the tuning widths of response fields were largely unaffected during FEF inactivation

$z = 0.0286$, Wilcoxon signed-rank test). Likewise, after performing an additional fit on FEF cool data using fixed parameters except for tuning width, we again found that tuning widths remained unchanged during FEF inactivation, although there was a trend toward decreasing widths of response fields ($p = 0.11$, $z = 1.6000$, Wilcoxon signed-rank test). While the small sample size hampered a detailed statistical analysis based on task, we obtained similar results compared to the pooled data except in that the largest decreases in peak spike count with FEF inactivation occurred in memory and delayed visually-guided saccade tasks. Together, the effects of FEF inactivation on the response field parameters of peak spike count and tuning width suggest that the overall spike count decreases throughout the entirety of the response field, regardless of saccade vector. While the horizontal position for the response field center did not change during FEF inactivation ($p = 0.69$, $z = -0.4000$, Wilcoxon signed-rank test), we did observe a significant upward bias for its vertical position ($p < 0.001$, $z = -3.4286$, Wilcoxon signed-rank test), although the magnitude of this change was quite small (0.2 mm, or 2.5 times smaller than the average tuning width of iSC neuron with a value of 0.5 mm). Given that FEF inactivation had no impact on the tuning widths of iSC response fields, this would seem to preclude the possibility that decreases in the cumulative spike count for metrically-matched saccades could be explained by additional spikes from the margins of the response field. Likewise, while modest vertical biases in iSC response fields during FEF inactivation was an unexpecting finding, such a mechanism by itself would not increase the overall spike count from the population of iSC neurons, as additional spikes for saccades toward the upper visual field would be offset by reductions for downward saccades. Overall, our results emphasize that FEF inactivation decreases the overall count of saccade-related spikes across the population of iSC neurons, and in doing so, provides evidence that the iSC is putting out fewer spikes regardless of saccade vector during FEF inactivation.

3.5 FEF inactivation altered the relationship between instantaneous spike count of iSC neurons and saccade displacement

A key notion within most models of the spatiotemporal transformation of saccades, including the dynamic linear ensemble-coding model, is that the FEF is simply an input to the iSC. If so, such a mechanism predicts that each iSC spike would be programmed to produce one fixed displacement mini-vector regardless of FEF inputs. However, this conflicts with how FEF inactivation decreased the overall number of iSC spikes regardless of saccade vector (*i.e.*, Fig. 5), hence we also tested this prediction by examining whether FEF inactivation altered the relationship between instantaneous spike count and saccade displacement. If FEF inactivation altered this relationship, then it provides further evidence to support our claim that the FEF has a more prominent role in the spatiotemporal transformation compared to simply providing cortical inputs to the iSC. Indeed, we found that FEF inactivation altered the relationship between instantaneous spike count and saccade displacement, whereby a similar displacement during the saccade trajectory was associated with a reduced number of iSC spikes during FEF inactivation.

For this analysis, we first plotted the instantaneous cumulative spike count as a function of saccade displacement from each trial (*i.e.*, no saccade matching procedure involved), then fit a linear regression across all trials from each iSC neuron. As shown in Fig. 6a using the previous example neuron, FEF inactivation reduced the slope of the regression, indicating that the iSC neuron fired less spikes for the same displacement vector during the saccade. Specifically, for this example neuron investigated with delayed visually-guided saccades, FEF inactivation decreased the regression slope from 0.62 to 0.56 ($p < 0.01$, $z = 3.1935$, Wilcoxon signed-rank test), but did not alter its intercept (0.9 unchanged, $p = 0.73$, $z = -0.3400$, Wilcoxon signed-rank test).

We found similar effects across our sample of iSC neurons studied in this task (right plot of Fig. 6a), as evidenced by the decreasing slope of the regression line

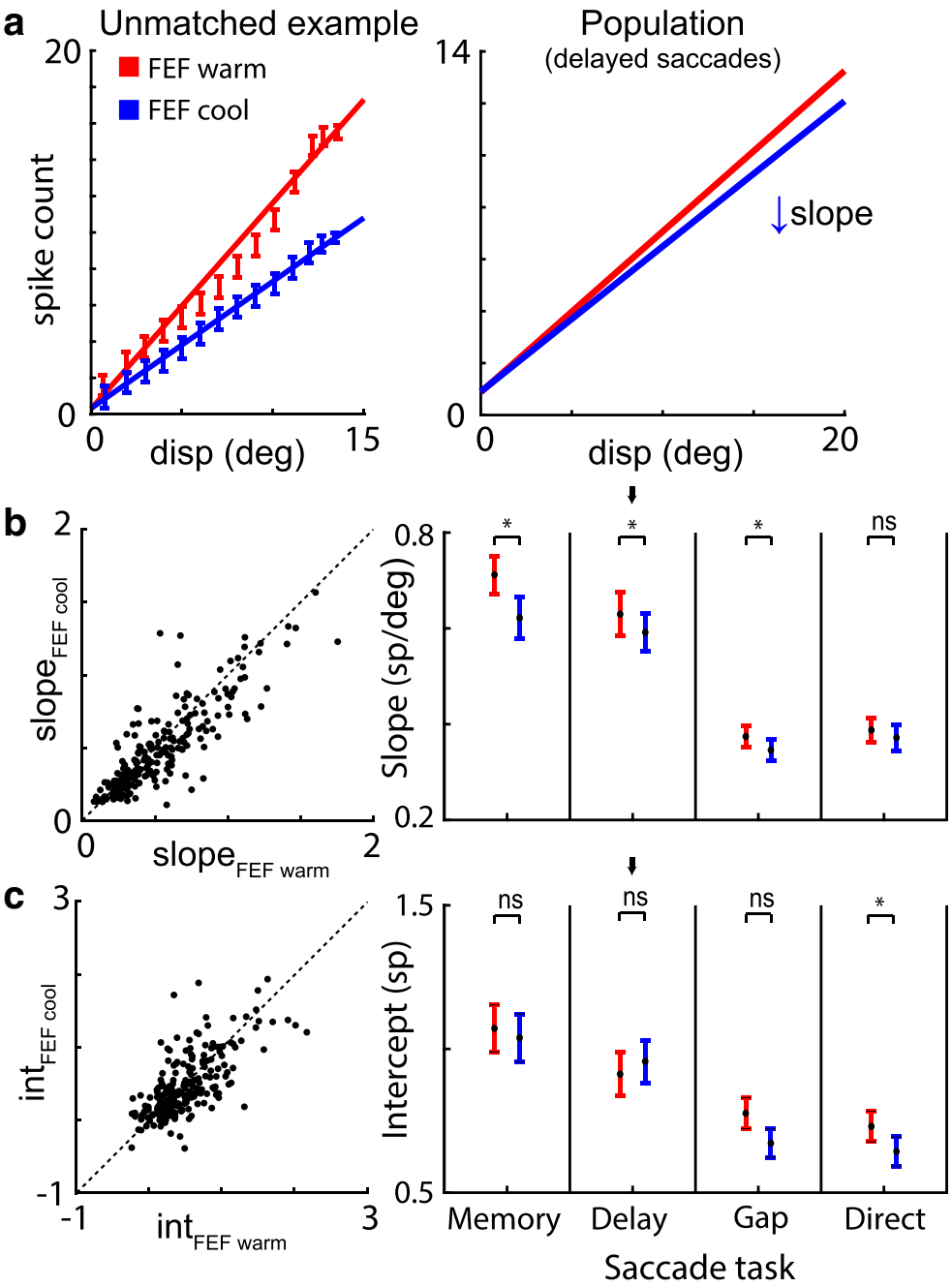

Fig. 6 FEF inactivation altered the relationship between cumulative spike count and saccade displacement within and across all iSC neurons. (**a**) Within our example neuron previously shown in Fig. 1a, but not matched for any saccade vectors, FEF inactivation reduced the average cumulative spike count per 1° of instantaneous displacement, such that this reduction was more pronounced at the end of the saccade. Bars indicate mean ± SD, using all instantaneous saccade displacements ±1° from each condition using a sliding window analysis. Independently, we also fitted a linear regression to all saccade trajectories within a single iSC neuron to quantify these changes. This analysis revealed a reduced slope without impacting the intercept of the relationship between cumulative spike count and saccade displacement**.** Critically, as shown on in right plot, this effect with FEF inactivation is consistently observed across all iSC neurons studied with the delayed, visually-guided task. (**b**) We observed consistent decreases in slopes, especially for more cognitively demanding tasks. Values are shown within each task in the right plot, where bars indicate mean ± SE across our sample (asterisk indicates significant effects between FEF warm and cool trials using a Wilcoxon rank sum test, $p < 0.05$). (**c**) In contrast, we observed no robust changes to intercept values in our sample of iSC neurons

computed from the average parameter values in the population. Across each saccade task, we observed robust changes in the slope with FEF inactivation for each neuron population, with more prominent effects in tasks with more cognitive demand. In particular, FEF inactivation caused a significant reduction in the regression slope except in the direct saccade task (Fig. 6b), with the overall slope value decreasing from 0.71 to 0.62, ($p < 10^{-14}$, z = 7.9132, Wilcoxon signed-rank test). In contrast, we observed no consistent influence of FEF inactivation on intercept values (Fig. 6c; 1.1 to 1.0, $p = 0.10$, z = 1.6573, Wilcoxon signed-rank test). Importantly, the influence of FEF inactivation on regression slopes could not be explained by the fitting procedure, given that r^2 values remained unchanged across all iSC neurons (0.64 to 0.61, $p = 0.09$, z = 1.6944, Wilcoxon signed-rank test). Together, our findings described up to this point demonstrate that the FEF likely has a role in the readout of iSC activity for the spatiotemporal transformation for saccades, especially in those cognitively-demanding tasks previously implicated with FEF function (Peel et al. 2014).

3.6 Changes in readout parameters in the dynamic linear ensemble-coding model are necessary to reconstruct matched saccades during FEF inactivation

Given that FEF inactivation likely alters the readout of iSC activity for saccade generation, we wondered which specific parameter within the model might explain our results. Recall that five fixed parameters are optimized within the model to reconstruct normal saccade dynamics using two linear feedback loops (Fig. 7a; γ_h and γ_v, respective scaling factors for each horizontal and vertical component based on projection strength, B, feedforward gain of saccade burst neurons, and τ and d, fixed delays of brainstem activation and of the feedback loops, respectively). For this analysis, we first optimized model parameters based on actual saccade dynamics within FEF warm trials of each task, and then compared how reconstructed saccades using these fixed model parameters could explain FEF cool trials having displacement-matched saccades (see **Methods** for more details). Subsequently, we also optimized certain model parameters within the FEF cool condition to examine whether changes in these parameters could more accurately reconstruct saccade dynamics (*i.e.*, displacement and velocity eye traces). Given our finding of fewer spikes emitting from the iSC during FEF inactivation, the model framework predicts a change in brainstem readout of iSC activity to correct for any differences in saccade displacement (see Fig. 7a). We hypothesized that a larger feedforward gain in the model could perhaps explain why fewer iSC spikes produced a similar saccade displacement with FEF inactivation.

The results from this analysis are shown in Fig. 7b for matched memory-guided saccades, which demonstrate that parameter changes in the model are required to fully account for any differences in iSC spikes and saccade trajectories during FEF inactivation. We found that such differences were apparent when we used the fixed FEF warm parameter values on FEF cool data, as the instantaneous number of iSC spikes is consistently lower during the saccade trajectory in the FEF cool data. Moreover, this analysis revealed that saccade trajectories were hypometric and reach lower peak velocities in FEF cool condition. These findings reaffirm our result that iSC neurons emit fewer spikes with FEF inactivation and the need to modify model parameters to account for differences between normal and reconstructed saccade dynamics. Importantly, when we optimized parameters based on FEF cool data, we found that increased scaling factors (by 1.2) and lowered feedforward gain (by 0.93) provided the best fit, such that it predicts that the iSC input to the brainstem should paradoxically increase with FEF inactivation.

This result is puzzling given that the scaling factor values are based on the anatomical projection strengths between the iSC and the premotor systems, and thus likely cannot change. Note that varying the time parameters (τ and d) almost always provided worse fits than those values obtained from FEF warm data, hence we limit our interpretation of our results to the other three parameters (γ_H, γ_V, B). We found similar paradoxical results within each task as shown in Fig. 6c, where usually optimizing both the scaling factors and feedforward gain were necessary to fully account for changes in saccade dynamics during FEF inactivation. In contrast, single parameter changes usually did not improve model fits, with the exception of increasing the scaling factor for memory-guided saccades. Collectively, these results suggest one mechanism by which the model accounts for differences in saccade dynamics during FEF inactivation, however does not provide a realistic alternative to our original prediction. This conclusion is especially pertinent given that the model does not include any pathway from the FEF to brainstem that bypasses the iSC, nor does it consider the likely contribution of the cerebellum on the brainstem circuitry.

3.7 Modifying the dynamic linear ensemble-coding model to include cerebellum-brainstem circuits may explain changes induced by FEF inactivation

To address these limitations, we wondered if modifying the model to include neurophysiological-plausible pathways could aid in the model framework, and thereby provide more tangible predictions about how FEF inactivation could alter the readout of iSC activity. While we acknowledge that this modification should be tested like the original model with blink-perturbed saccades, the purpose of this modified model was to simply reconcile our paradoxical findings and provide tangible predictions for future neurophysiology experiments. We explicitly explored the modified model as depicted in Fig. 8a, which retains the two horizontal and vertical premotor systems, but moves both feedback comparators to the midbrain NRTP whereby a single comparator may influence (*via* the cerebellum) the feedforward gains in a non-spatially selective manner. Evidence for this modification stems from both the iSC and the FEF having projections to the cerebellum *via* the NRTP (Quaia et al. 1999), which in turn is known to participate in feedbacks loops involving the neural integrators. Moreover, there is a lack of evidence for a neuronal comparator within the premotor systems (Smalianchuk et al. 2018) and the long-lead burst neurons that drive the excitatory bust neurons likely do not contain sufficient local feedback to maintain an integrated sum of all iSC spikes. It is also important to recognize the role of the oculomotor vermis within the cerebellum, which in the modified model receives NRTP input and adds an offset to the gain signal, such that the cerebellum output area, the cFN, provides a compensatory gain on the excitatory burst neurons. We predicted that this variable output from the cerebellum could provide a possible substrate for how FEF inactivation influences the readout of iSC activity, which we tested using our dataset following a similar procedure as we did with the original model (*i.e.*, Fig. 7).

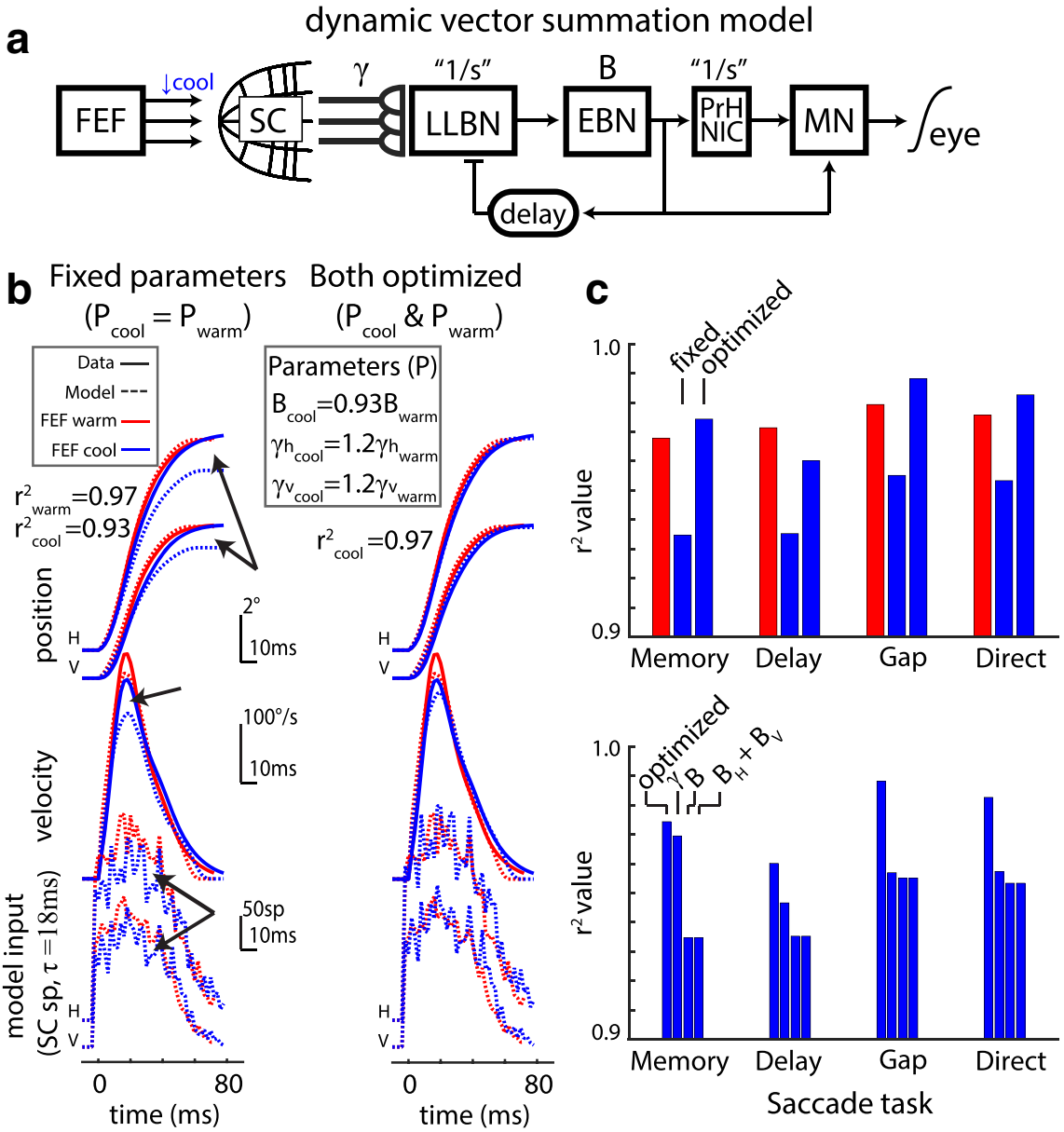

Fig. 7 FEF inactivation alters the readout of iSC activity in a brainstem implementation of the dynamic linear ensemble-coding model. (**a**) A schematic of the dynamic linear ensemble-coding model that contains the γ_h, γ_v, B, τ and d parameters (see **Methods** for full description). We predicted that the brainstem readout of iSC spikes is altered during FEF inactivation, otherwise it would produce differences in saccade dynamics, including saccadic hypometria. Note that only one of two linear feedback loops (*i.e.*, separate horizontal and vertical premotor systems) are shown, and the signal transformation for the eye plant is not shown but included in the model. 1/s represents neuronal integration using Laplace notation. LLBN, long-lead burst neurons; EBN, excitatory burst neurons; PrH, nucleus prepositus hypoglossus; NIC, interstitial nucleus of Cajal; MN, motoneurons. (**b**) The "fixed" parameter values optimized for FEF warm trials in the memory-guided saccade task were not sufficient to accurately reconstruct the average saccade trajectory with FEF inactivation. For this analysis, we used trials having displacement matched saccades, hence saccade displacements should be equivalent with and without FEF inactivation. The shown model input for the horizontal and vertical feedback loops is the instantaneous spike count across iSC neurons (2 ms bins following a delay of τ = 18 ms), which is scaled by the γ_h and γ_v parameter, respectively (see **Methods** for details). Importantly, independently optimizing model parameters for FEF warm and cool trials produced near perfect fits, such that increasing the horizontal and vertical scaling factors minimized any differences in estimated iSC activity or saccade dynamics. (**C**) We found similar trends across matched FEF warm and cool trials in all four saccade tasks. In each case, usually optimizing multiple parameters to FEF cool data, rather than use fixed FEF warm values, could produce similar fits to saccade trajectories (top). One slight exception is for memory-guided saccades, whereby an equal proportional increase to the horizontal and vertical scaling factors alone (γ) provided a good fit to FEF cool data (bottom). Note that "$B_H + B_V$"condition indicates optimizing the feedforward gain parameter separately for horizontal and vertical premotor systems

Indeed, we found that these biologically-plausible modifications to the model provide a viable alternative mechanism for how FEF inactivation influences saccade dynamics. For example, as shown for matched memory-guided saccades in Fig. 8b, the modified model can reconstruct equivalent saccade trajectories during FEF inactivation through adjustments to only two parameters associated with cerebellum output to the brainstem. In particular, we found increasing the gain offset of cerebellum output (increase ε by factor of 1.7 compared to FEF warm) and decreasing NRTP input (decrease α by 0.8 compared to FEF warm) in the modified model for FEF cool trials was sufficient to produce similar saccade dynamics compared to matched FEF warm trials. Such parameter modifications would be consistent with our original prediction whereby an increase to the feedforward gain in each premotor system (*i.e.*, excitatory burst neurons) compensates for reduced iSC spikes during FEF inactivation, and it also identifies a possible mechanism for how the FEF might influence the spatiotemporal transformation independent of iSC activity. Importantly, we found similar results across all four tasks we studied (Fig. 8c), albeit the model framework could sufficiently explain FEF cool data without any parameter changes in the gap saccade task. Moreover, the α term necessary to explain FEF cool data decreased for more cognitively demanding tasks, possibly identifying a link between how FEF activity might influence saccade dynamics precisely in those tasks for which it is involved. Together, this approach using modified framework of the linear dynamic ensemble-coding model suggests that cerebellum-brainstem circuits might play an important role in the spatiotemporal transformation, particularly when FEF integrity is compromised.

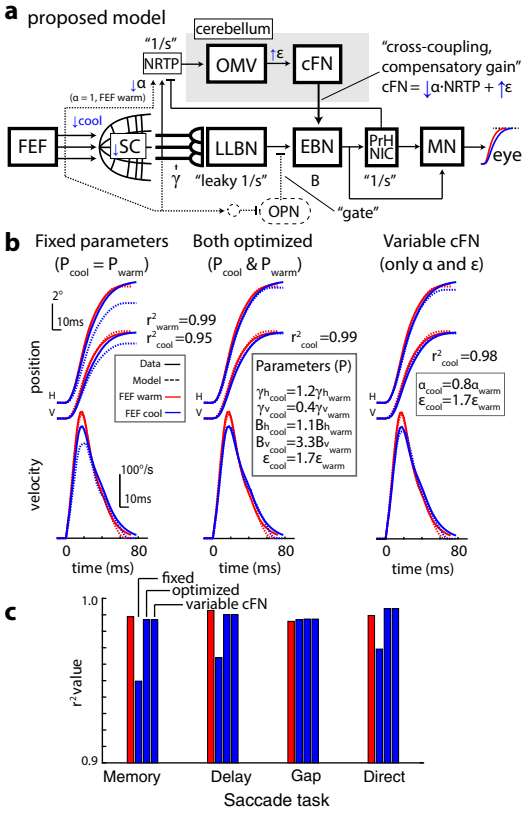

Fig. 8 A potential mechanism to explain the altered readout of iSC activity with FEF inactivation: a compensatory influence of the cerebellum on the feedforward gain. (**a**) Proposed model which is a modification of the brainstem implementation of the dynamic linear ensemble-coding model (see **Methods** for full description). In particular, we incorporated a new pathway arising from the iSC to the brainstem through the cerebellum, which could influence the feedforward gain in the brainstem, and in doing so can provide a more robust explanation to changes in model parameters with FEF inactivation. Note that dashed lines indicate speculated pathways that clarify our interpretation of results, but are not explicitly part of the modified model. NRTP, nucleus reticularis tegmenti pontis; OMV, oculomotor vermis; cFN, caudal fastigial nucleus. (**b**) Similar to the original model in Fig. 7b, the new implementation of model required adjustments to model parameters (γ_h, γ_v, B_h, B_v, and ε) to reconstruct matched memory-guided saccades during FEF inactivation. However, note that modifying only two parameters related to cerebellum function (α and ε) sufficiently explained FEF cool data, suggesting a mechanism by which the cerebellum could influence the brainstem readout of iSC activity. (**c**) Across all our saccade tasks, modifying only the cerebellum's influence on the feedforward gain in both horizontal and vertical premotor systems sufficiently explained FEF cool data

4 Discussion

The saccadic spatiotemporal transformation is traditionally viewed as a function of the oculomotor brainstem, occurring between the iSC and the downstream burst generator (Groh 2001; Moschovakis et al. 1998; Scudder et al. 2002). The linear dynamic ensemble-coding model proposed by Goossens and Van Opstal (2006) incorporates this view, relegating the role of cortical inputs like the FEF to specification of saccade goal, which is then executed by the iSC and burst generator without cortical involvement. We tested a core prediction of this model using reversible FEF inactivation: if the saccade displacement vector is the same, then the overall number of iSC spikes should be equivalent during FEF inactivation. Instead, we found that FEF inactivation reduced the number of iSC spikes for displacement-matched saccades, both at the center and throughout the entirety of the movement field, doing so in a task-dependent manner. Fundamentally, the iSC emits fewer spikes for displacement-matched saccades during FEF inactivation, and FEF inactivation somehow alters the readout of each iSC spike to produce a larger displacement mini-vector. In the following sections, we discuss the implications of our results from the perspective of the model, and from the perspective of how the oculomotor system may instantiate the spatiotemporal transformation.

4.1 A task-dependent role for the FEF in the spatiotemporal transformation

Our four tasks varied the need to delay a response and remember the location of the peripheral target. We found that the

decrease of saccade-related iSC spikes for metrically-matched saccades during FEF inactivation scaled with the cognitive demands of the task, with the greatest decrease accompanying memory-guided saccades that required a delayed response to a remembered target location and the smallest decrease accompanying direct saccades that required an immediate response to a persistently visible target. These task-dependent effects mirror the impact of FEF inactivation in more cognitively-demanding saccade tasks (Dias and Segraves 1999; Peel et al. 2014; Sommer and Tehovnik 1997). Further, we found that the spatial distribution of saccade-related iSC activity did not change during FEF inactivation. These results could not have been foreseen, as the decreases in iSC spike frequency during FEF inactivation that accompany lower saccade velocities (Peel et al. 2017) could have been offset by increases in saccade duration to yield a fixed number of spikes. Inputs to the iSC from extra-tectal sources also persist during FEF inactivation, but any compensatory changes in such inputs, in conjunction with intrinsic circuits within the iSC, are apparently insufficient to ensure a fixed number of iSC spikes during FEF inactivation.

Van Opstal and colleagues tested the linear dynamic ensemble coding model using a perturbation approach where a blink was induced just prior to a direct visually-guided saccade (Goossens and Van Opstal 2000a). They found that the iSC continued to emit a fixed number of spikes despite remarkably perturbed saccadic trajectories (Goossens and Van Opstal 2006). In contrast, we find that the number of iSC spikes changes during FEF inactivation, despite relatively modest decreases in saccade velocity and a straight saccade trajectory. We speculate that the differences in results arising from blink-perturbation *versus* FEF inactivation relate to the level at which each perturbation influences brain function. In contrast with direct manipulation of cortical activity *via* cryogenics, the trigeminal blink reflex appears to interact with iSC activity within less than 10 ms, presumably *via* subcortical trigiminotectal, cerebellotectal, or nigrotectal pathways, and also influences saccade trajectory *via* influences exerted downstream of the iSC (Goossens and Van Opstal 2000b).

Previous studies on the linear dynamic ensemble coding model relied on saccades made directly to presented targets (Goossens and Van Opstal 2006, 2012). Our warm-to-warm comparison, which established the noise inherent to our saccade matching procedure, shows that iSC neurons emits a fixed number of spikes for metrically-matched saccades in all paradigms, including memory and delayed visually-guided saccades. Unfortunately, the majority of our neurons were only tested in a single behavioural task, given our specific focus on FEF inactivation. Given the task-dependent nature of our results, a future test for the linear dynamic ensemble coding model will be to determine whether a given iSC neuron emits a fixed number of spikes throughout a response field for metrically-matched saccades generated in different paradigms with varying degrees of cognitive involvement (*e.g.*, comparing direct *versus* delayed visually-guided saccades, or pro- *versus* anti-saccades). Doing so would clarify the contributions of extra-tectal sources to saccadic control across a variety of tasks.

4.2 An increased feedforward gain may counteract decreased iSC activity for metrically-matched saccades

Our results lead us to speculate as to what modifications to the linear dynamic ensemble-coding model would be required to explain the effects of FEF inactivation. Within the model, each iSC spike is applied independently (see Eq. 1 in **Methods**), so that the brainstem burst generator evokes a saccade commanded by the summed mini-vectors associated with each iSC spike. The model proposes that iSC activity is read out by the brainstem circuitry by a total of five parameters (scaling factors for horizontal and vertical component based on projection strength, feedforward gain of saccade burst neurons, and fixed delays of brainstem activation and of the feedback loops). The implication of fewer iSC spikes for metrically-matched saccades during FEF inactivation is that the impact of each spike would have to be, somewhat paradoxically, greater. Of the five parameters, the simplest explanation of our results is that FEF inactivation increases the feedforward gain of saccade burst neurons in the brainstem, doing so in a task-dependent manner. Unfortunately, this explanation is not consistent from the model when using FEF warm and cool trials having displacement matched saccades. Specifically, the current model framework suggested that increasing the scaling factors and decreasing the feedforward gain better reflected the changes during FEF inactivation. Nonetheless, such changes to scaling factors seem less likely for a variety of reasons. The horizontal and vertical scaling factors are based on a nonlinear representation of visual space within the iSC (Robinson 1972) that presumably relate to projection strengths with the brainstem (Moschovakis et al. 1998; Ottes et al. 1986); it seems unlikely that these projection strengths could change suddenly during FEF inactivation. Further, as we found that FEF inactivation reduced iSC spike counts within varying time windows, it is not immediately obvious how changes in delay parameters could counteract the decreased number of iSC spikes arriving at the brainstem burst generator. In fact, varying these time parameters almost always did not improve data fits compared to those obtained with an intact FEF. Thus, the current model framework appears limited in its ability to explain how FEF inactivation can influence the readout of iSC activity.

To explain this paradoxical finding, we also modified the linear dynamic ensemble-coding model based on available neurophysiological evidence, which provided one robust mechanism for our results. Namely, adding a second pathway from the iSC to the brainstem *via* the cerebellum, and moving the comparators from the premotor systems to the midbrain NRTP that relays iSC

signals to the cerebellum. Interestingly, we obtained good fits with FEF inactivation from changing only two parameters relating to this cerebellum-brainstem pathway in the modified model, and the magnitude of these changes also varied with the task demands. These parameter changes to the cerebellum-brainstem pathway primarily acted to provide a gain offset during FEF inactivation, which increased both the horizontal and vertical feedforward gain within the model. Importantly, our results obtained with this modified model provide a viable mechanism for how the FEF can influence the spatiotemporal transformation of saccades, and in doing so provide testable predictions about the role of downstream oculomotor areas for future studies to address.

4.3 Neurophysiological implications for the spatiotemporal transformation

Although the spatiotemporal transformation for saccades is traditionally viewed as a function of the oculomotor brainstem (Groh 2001; Moschovakis et al. 1998; Scudder et al. 2002), the work of Schiller et al. (1980) showed that monkeys with SC ablations generate accurate saccades after a period of recovery, so long as the FEF was intact. Given that the FEF, like the iSC, represents saccade targets in a spatial reference frame, these results demonstrate that the spatiotemporal transformation can occur between the FEF and oculomotor brainstem in the absence of the iSC, after a period of recovery. Much remains to be learned about the role of signalling conveyed along the FEF pathway that bypasses the iSC, although this pathway is not sufficient to evoke saccades in the intact animal (Hanes and Wurtz 2001). Regardless, our results are inconsistent with a straightforward idea that FEF signals duplicate what is issued by the iSC. Indeed, had FEF spikes also provided mini-vectors that sum with those from the iSC, then one could have predicted that more, not fewer, iSC spikes would have been required during FEF inactivation for metrically-matched saccades. Instead, our results suggest that FEF and iSC signals to the brainstem circuitry have unique contributions to the spatiotemporal transformation in an intact animal. This perspective complements findings from previous studies suggesting that the FEF and iSC monosynaptically connect with different regions within the oculomotor brainstem: neurons from the caudal iSC excite saccadic burst neurons within the paramedian pontine reticular formation at monosynaptic latencies (Raybourn and Keller 1977), whereas FEF corticopontine neurons terminate within the brainstem region containing the omni-pause neurons (OPNs) (Segraves 1992).

There are multiple potential mechanisms by which FEF inactivation could influence the readout of iSC activity. As previously mentioned, we speculate that one explanation for our results could be that the cerebellum compensates for reduced FEF function, such that it ultimately increases the feedforward gain of both premotor systems. Hence, it would also be very interesting to assess the impact of FEF inactivation on signaling conveyed to and within the cerebellum (Huerta et al. 1986; Xiong et al. 2002) given its widespread connections with the oculomotor brainstem and role in influencing saccade amplitude (Fuchs et al. 1993; Sato and Noda 1992). We predict that the oculomotor vermis might be a substrate for this compensatory gain change with FEF inactivation, by the recruitment of more cFN neurons projecting to the excitatory burst neurons.

Another explanation for our results could be that FEF inactivation decreases the tonic level of OPN activity during stable fixation, which activity is tightly correlated with eye movement velocity (Yoshida et al. 1999). This mechanism is based on our observations that FEF inactivation decreases all aspects of functionally-defined ipsilesional iSC emanating from both the rostral and caudal iSC (Dash et al. 2018; Peel et al. 2017), and ideas on how OPNs receive scaled excitatory inputs from the rostro-caudal extent of the iSC (Everling et al. 1998; Gandhi and Keller 1997). Given the mutually-antagonistic relationship between OPN and burst neuron firing, such a decrease in OPN activity may lead to proportionate disinhibition of the brainstem burst generator, which could be the correlate of an increase in feedforward gain. Presumably any functional compensation following FEF inactivation that acts to decrease OPN activity was indirect as current evidence of the direct FEF pathways to the OPN region (Segraves 1992) predicts that FEF inactivation would result in increased OPN activity. This prediction is based on electrical stimulation of the FEF pathway to the OPN region causing decreased OPN firing rates *via* an inhibitory interneuron, consistent with the FEF having a role in silencing OPN activity to allow for saccade generation. However, it should be also be noted that OPNs can also have an excitatory influence on EBNs due to its neurotransmitter glycine (Miura and Optican 2006), which can explain why OPN inactivation causes saccadic slowing (Soetedjo et al. 2002). Hence further study is needed to determine the various mechanisms by which OPNs alter the feedforward gain of the EBNs for saccade generation, as well as, whether direct FEF connections to the OPN play a significant functional role.

Collectively, these compensatory mechanisms might also provide insights into how the oculomotor system adapts following basal ganglia degeneration (*i.e.* Parkinson's disease), which patients exhibit hypometria and prolonged saccade durations (Anderson and MacAskill 2013), analogous to the effects of FEF inactivation. Fortunately, this study provides a foundation for future recordings in the OPNs, cerebellum, and basal ganglia during FEF inactivation, permitting new ways to test and refine biologically-plausible models for signal transformations within the oculomotor system.

Acknowledgements This work was supported by operating grants from the Canadian Institutes of Health Research to BDC (MOPs: 93796, 123247 and 142317) and the Natural Sciences and Engineering Research Council (NSERC; RGPIN-311680). TRP was supported by an Ontario Graduate Scholarship and TRP and SD were supported by funding from an NSERC CREATE grant.

Compliance with ethical standards

Conflict of interest The authors declare no conflict of interest.

References

Anderson, T. J., & MacAskill, M. R. (2013). Eye movements in patients with neurodegenerative disorders. Nature Reviews Neurology. Nature Publishing Group.

Barash, S., Bracewell, R. M., Fogassi, L., Gnadt, J. W., & Andersen, R. A. (1991). Saccade-related activity in the lateral intraparietal area. I. Temporal properties; comparison with area 7a. *Journal of Neurophysiology, 66*(3), 1095–1108.

Bruce, C. J., & Goldberg, M. E. (1985). Primate frontal eye fields .I. Single neurons discharging before saccades. *Journal of Neurophysiology, 53*(3), 603–635.

Crapse, T. B., & Sommer, M. A. (2009). Frontal eye field neurons with spatial representations predicted by their subcortical input. *The Journal of neuroscience : the official journal of the Society for Neuroscience, 29*(16), 5308–5318.

Dash, S., Peel, T. R., Lomber, S. G., & Corneil, B. D. (2018). Frontal eye field inactivation reduces saccade preparation in the superior Colliculus but does not Alter how preparatory activity relates to saccades of a given latency. *eNeuro*, *5*(2), ENEURO.0024-18.2018.

Deng, S.-Y., Goldberg, M., Segraves, M., Ungerleider, L., & Mishkin, M. (1986). The effect of unilateral ablation of the frontal eye fields on saccadic performance in the monkey. In E.L. Keller, \D.S. Zee, (Eds.), Adaptive processes in the visual and oculomotor systems. (pp. 201–208). Oxford: Pergamon Press.

Dias, E. C., & Segraves, M. A. (1999). Muscimol-induced inactivation of monkey frontal eye field: Effects on visually and memory-guided saccades. *Journal of Neurophysiology, 81*(5), 2191–2214.

Everling, S., Paré, M., Dorris, M. C., & Munoz, D. P. (1998). Comparison of the discharge characteristics of brain stem Omnipause neurons and superior Colliculus fixation neurons in monkey: Implications for control of fixation and saccade behavior. *Journal of Neurophysiology, 79*(2), 511–528.

Fuchs, A. F., Robinson, F. R., & Straube, A. (1993). Role of the caudal fastigial nucleus in saccade generation. I. Neuronal discharge pattern. *Journal of Neurophysiology, 70*(5), 1723–1740.

Gandhi, N. J., & Katnani, H. A. (2011). Motor functions of the superior Colliculus. *Annual Review of Neuroscience, 34*(1), 205–231.

Gandhi, N. J., & Keller, E. L. (1997). Spatial distribution and discharge characteristics of superior Colliculus neurons Antidromically activated from the Omnipause region in monkey. *Journal of Neurophysiology, 78*(4), 2221–2225.

Goossens, H. H. L. M., & Van Opstal, A. J. (2000a). Blink-perturbed saccades in monkey. I. Behavioral Analysis. *Journal of Neurophysiology, 83*(6), 3411–3429.

Goossens, H. H. L. M., & Van Opstal, A. J. (2000b). Blink-perturbed saccades in monkey. . II. Superior Colliculus Activity. *Journal of Neurophysiology, 83*(6), 3430–3452.

Goossens, H. H. L. M., & Van Opstal, A. J. (2006). Dynamic ensemble coding of saccades in the monkey superior Colliculus. *Journal of Neurophysiology, 95*(4), 2326–2341.

Goossens, H. H. L. M., & Van Opstal, A. J. (2012). Optimal control of saccades by spatial-temporal activity patterns in the monkey superior Colliculus. *PLoS Computational Biology, 8*(5), e1002508.

Groh, J. M. (2001). Converting neural signals from place codes to rate codes. *Biological Cybernetics, 85*(3), 159–165.

Hafed, Z. M., & Chen, C.-Y. (2016). Sharper, stronger, faster upper visual field representation in primate superior Colliculus. *Current Biology, 26*(13), 1647–1658.

Hanes, D. P., & Wurtz, R. H. (2001). Interaction of the frontal eye field and superior colliculus for saccade generation. *Journal of Neurophysiology, 85*(2), 804–815.

Hikosaka, O., Takikawa, Y., & Kawagoe, R. (2000). Role of the basal ganglia in the control of purposive saccadic eye movements. *Physiological Reviews, 80*(3), 953–978.

Huerta, M. F., Krubitzer, L. A., & Kaas, J. H. (1986). Frontal eye field as defined by intracortical microstimulation in squirrel monkeys, owl monkeys, and macaque monkeys: I. subcortical connections. *The Journal of Comparative Neurology, 253*(4), 415–439.

Kasap, B., & Van Opstal, A. J. (2017). A spiking neural network model of the midbrain superior colliculus that generates saccadic motor commands. *Biological Cybernetics, 111*(3–4), 249–268.

Kasap, B., & Van Opstal, A. J. (2019). Microstimulation in a spiking neural network model of the midbrain superior colliculus. *PLoS Computational Biology, 15*(4), e1006522.

Keating, E. G., & Gooley, S. G. (1988). Saccadic disorders caused by cooling the superior colliculus or the frontal eye field, or from combined lesions of both structures. *Brain Research, 438*(1–2), 247–255.

Lomber, S. G., Payne, B. R., & Horel, J. A. (1999). The cryoloop: An adaptable reversible cooling deactivation method for behavioral or electrophysiological assessment of neural function. *Journal of Neuroscience Methods, 86*(2), 179–194.

McPeek, R. M., & Keller, E. L. (2002). Saccade target selection in the superior colliculus during a visual search task. *Journal of Neurophysiology, 88*(4), 2019–2034.

Miura, K., & Optican, L. M. (2006). Membrane channel properties of premotor excitatory burst neurons may underlie saccade slowing after lesions of omnipause neurons. *Journal of Computational Neuroscience, 20*(1), 25–41.

Moschovakis, A. K., Kitama, T., Dalezios, Y., Petit, J., Brandi, A. M., & Grantyn, A. A. (1998). An anatomical substrate for the spatiotemporal transformation. *The Journal of neuroscience : the official journal of the Society for Neuroscience, 18*(23), 10219–10229.

Munoz, D. P., & Wurtz, R. H. (1995). Saccade-related activity in monkey superior colliculus. I. Characteristics of burst and buildup cells. *Journal of Neurophysiology, 73*(6), 2313–2333.

Nichols, M. J., & Sparks, D. L. (1996). Component stretching during oblique stimulation-evoked saccades: The role of the superior colliculus. *Journal of Neurophysiology, 76*(1), 582–600.

Ottes, F. P., Van Gisbergen, J. A. M., & Eggermont, J. J. (1986). Visuomotor fields of the superior colliculus: A quantitative model. *Vision Research, 26*(6), 857–873.

Peel, T. R., Dash, S., Lomber, S. G., & Corneil, B. D. (2017). Frontal eye field inactivation diminishes superior Colliculus activity, but delayed saccadic accumulation governs reaction time increases. *The Journal of neuroscience : the official journal of the Society for Neuroscience, 37*(48), 11715–11730.

Peel, T. R., Hafed, Z. M., Dash, S., Lomber, S. G., & Corneil, B. D. (2016). A causal role for the cortical frontal eye fields in microsaccade deployment. *PLoS Biology, 14*(8), e1002531.

Peel, T. R., Johnston, K., Lomber, S. G., & Corneil, B. D. (2014). Bilateral saccadic deficits following large and reversible inactivation of unilateral frontal eye field. *Journal of Neurophysiology, 111*(2), 415–433.

Quaia, C., Lefèvre, P., & Optican, L. M. (1999). Model of the control of saccades by superior colliculus and cerebellum. *Journal of Neurophysiology, 82*(2), 999–1018.

Raybourn, M. S., & Keller, E. L. (1977). Colliculoreticular organization in primate oculomotor system. *Journal of Neurophysiology, 40*(4), 861–878.

Robinson, D. A. (1972). Eye movements evoked by collicular stimulation in the alert monkey. *Vision Research, 12*(11), 1795–1808.

Sato, H., & Noda, H. (1992). Saccadic dysmetria induced by transient functional decortication of the cerebellar vermis. *Experimental Brain Research, 88*(2), 455–458.

Schiller, P. H., True, S. D., & Conway, J. L. (1980). Deficits in eye movements following frontal eye-field and superior colliculus ablations. *Journal of Neurophysiology, 44*(6), 1175–1189.

Scudder, C. A., Kaneko, C. R., & Fuchs, A. F. (2002). The brainstem burst generator for saccadic eye movements: A modern synthesis. *Experimental Brain Research, 142*(4), 439–462.

Segraves, M. A. (1992). Activity of monkey frontal eye field neurons projecting to oculomotor regions of the pons. *Journal of Neurophysiology, 68*(6), 1967–1985.

Smalianchuk, I., Jagadisan, U. K., & Gandhi, N. J. (2018). Instantaneous midbrain control of saccade velocity. *Journal of Neuroscience, 38*(47), 10156–10167.

Soetedjo, R., Kaneko, C. R. S., & Fuchs, A. F. (2002). Evidence that the superior colliculus participates in the feedback control of saccadic eye movements. *Journal of Neurophysiology, 87*(2), 679–695.

Sommer, M. A., & Tehovnik, E. J. (1997). Reversible inactivation of macaque frontal eye field. *Experimental Brain Research, 116*(2), 229–249.

Sparks, D. L. (1986). Translation of sensory signals into commands for control of saccacid eye movements: Role of primate superior colliculus. *Physiological Reviews, 66*, 118–171.

Sparks, D. L., & Mays, L. E. (1990). Signal transformations required for the generation of saccadic eye movements. *Annual Review of Neuroscience, 13*(1), 309–336.

Sparks, D. L. (2002). The brainstem control of saccadic eye movements. *Nature Reviews Neuroscience, 3*(12), 952–964.

Thompson, K. G., Hanes, D. P., Bichot, N. P., & Schall, J. D. (1996). Perceptual and motor processing stages identified in the activity of macaque frontal eye field neurons during visual search. *Journal of Neurophysiology, 76*(6), 4040–4055.

Van der Willigen, R. F., Goossens, H. H. L. M., & Van Opstal, A. J. (2011). Linear visuomotor transformations in midbrain superior colliculus control saccadic eye movements. *Journal of Integrative Neuroscience, 10*(03), 277–301.

Van Opstal, A. J., & Goossens, H. H. L. M. (2008). Linear ensemble-coding in midbrain superior colliculus specifies the saccade kinematics. *Biological Cybernetics, 98*(6), 561–577.

Van Opstal, A. J., & Van Gisbergen, J. A. M. (1989). A nonlinear model for collicular spatial interactions underlying the metrical properties of electrically elicited saccades. *Biological Cybernetics, 60*(3), 171–183.

White, B. J., & Munoz, D. P. (2011). The superior colliculus. In S. P. Liversedge, I. Gilchrist, & S. Everling (Eds.), *The Oxford Handbook of Eye Movements* (pp. 195–214). Oxford University Press.

Wurtz, R. H., Sommer, M. A., Paré, M., & Ferraina, S. (2001). Signal transformations from cerebral cortex to superior colliculus for the generation of saccades. *Vision Research, 41*(25–26), 3399–3412.

Xiong, G., Hiramatsu, T., & Nagao, S. (2002). Corticopontocerebellar pathway from the prearcuate region to hemispheric lobule VII of the cerebellum: An anterograde and retrograde tracing study in the monkey. *Neuroscience Letters, 322*(3), 173–176.

Yoshida, K., Iwamoto, Y., Chimoto, S., & Shimazu, H. (1999). Saccade-related inhibitory input to pontine omnipause neurons: An intracellular study in alert cats. *Journal of Neurophysiology, 82*(3), 1198–1208.